Published in final edited form as:
Toxicology. 2021 June 30; 458: 152823. doi:10.1016/j.tox.2021.152823.

The Dynamicity of Acute Ozone-Induced Systemic Leukocyte Trafficking and Adrenal-Derived Stress Hormones

Andres R. Henriquez[a,*], **Wanda Williams**[b], **Samantha J. Snow**[b,*], **Mette C. Schladweiler**[b], **Cynthia Fisher**[c], **Marie M. Hargrove**[a,*], **Devin Alewel**[a], **Catherine Colonna**[a], **Stephen H. Gavett**[b], **Colette N. Miller**[b], **Urmila P. Kodavanti**[b,**]

[a]Oak Ridge Institute for Science and Education, Research Triangle Park, North Carolina, United States of America

[b]Public Health and Integrated Toxicology Division, Center for Public Health and Environmental Assessment, U.S. Environmental Protection Agency, Research Triangle Park, North Carolina, United States of America

[c]School of Public Health, University of North Carolina, Chapel Hill, NC 27599

Abstract

Ozone exposure induces neuroendocrine stress response, which causes lymphopenia. It was hypothesized that ozone-induced increases in stress hormones will temporally follow changes in circulating granulocytes, monocytes and lymphocyte subpopulations. The goal of this study was to chronicle the changes in circulating stress hormones, cytokines, and leukocyte trafficking during 4-hour exposure to ozone. Male Wistar Kyoto rats were exposed to air or ozone (0.4 or 0.8 ppm) for 0.5, 1, 2, or 4 hours. After each time point, Circulating stress hormones and cytokines, and lung gene expression were assessed along with live and apoptotic granulocytes, monocytes (classical and non-classical), and lymphocytes (B, T_h and T_c) in blood, thymus and spleen using flow cytometry. Circulating stress hormones began to increase at 1 hour of ozone exposure. Lung expression of inflammatory cytokines (*Cxcl2*, *Il6*, and *Hmox1*) and glucocorticoid-responsive genes (*Nr3c1*, *Fkbp5* and *Tsc22d3*) increased in both a time- and ozone concentration-dependent manner. Circulating granulocytes increased at 0.5 hours of ozone exposure but tended to decrease at 2 and 4 hours, suggesting a rapid egress and then margination to the lung. Classical monocytes decreased over 4 hours of exposure periods (~80% at 0.8 ppm). B and T_c lymphocytes significantly decreased after ozone exposure at 2 and 4 hours. Despite dynamic shifts in circulating immune cell populations, few differences were measured in serum cytokines. Ozone neither increased apoptotic cells nor altered thymus and spleen lymphocytes.

Address correspondence to: Urmila P. Kodavanti, PhD, MD B105-02, PHITD, CPHEA, US EPA, Research Triangle Park, NC 27711, kodavanti.urmila@epa.gov, Phone: 919 541-4963; Fax: 919-541-0026.
*Current addresses:
SJS: ICF International Inc., Durham, North Carolina, United States of America
MM: Syngenta, Greensboro, North Carolina, United States of America

Author Declaration: The authors declare no competing interests.

Disclaimer: The research described in this article has been reviewed by the Center for Public Health and Environmental Assessment, U.S. Environmental Protection Agency, and approved for publication. Approval does not signify that the contents necessarily reflect the views and policies of the Agency, nor does the mention of trade names of commercial products constitute endorsement or recommendation for use.

The data show that ozone-induced increases in adrenal-derived stress hormones precede the dynamic migration of circulating immune cells, likely to the lung to mediate inflammation.

Keywords

Inhaled pollutants; stress hormones; neuroendocrine; immune response; classical monocytes; circulating lymphocytes; lung

1. INTRODUCTION

As of 2017, air pollution is considered the fourth greatest risk factor in human mortality (Ritchie and Roser, 2020), contributing to nearly 70% of all environmental causes (Landrigan et al., 2018). Despite decades of research on how air pollution affects pulmonary and cardiovascular systems (U.S. EPA., 2020), the understanding of how systemic effects are initiated once the lung encounters inhaled pollutants is still lacking. There has been even less research on the systemic immune effects of air pollutants (Steenhof et al., 2014; Francis et al., 2017), and the mechanisms by which circulating mediators promote peripheral immune response after air pollution exposure remain unclear (Scapellato and Lotti, 2007; Münzel et al., 2017). It is believed that cytokines and reactive intermediates released into the circulation upon lung injury from air pollution exposure mediate systemic and extrapulmonary effects, however, data are lacking or inconsistent to support this assertion. It is also not understood what initiates the innate immune response that occurs hours after a single air pollution exposure.

Innate and adaptive immune systems are activated in response to an injury or pathogen encounter leading to bone marrow pluripotent hematopoietic stem cell differentiation, maturation and egress (Nicholson, 2016; Krausgruber et al., 2020). The myeloblast-derived monocytes and granulocytes are involved in innate immune response that occur rapidly as a first line of defense after injury or pathogen encounter (Gasteiger et al., 2017). During this time the adaptive immune response is also stimulated involving bone marrow-derived lymphoid stem cell differentiation and maturation to B and T lymphocytes, and natural killer cells in lymphoid organs. The timing of stress signals to the brain, their intensity, characteristics, and location govern where, and how the innate immune response is directed and its longevity, which are critical for host survival. This stress response orchestrated by the neuroendocrine system has been well established, however these pathways have not been linked to air pollution-induced inflammation and changes in immune organs until recently (Henriquez et al., 2018).

The neuroendocrine system is critical in mediating pulmonary inflammation and systemic effects after exposure to ozone (Snow et al., 2018; Kodavanti 2019). Specifically, it has been shown that in rats a single ozone exposure activates the sympathetic-adrenal-medullary (SAM) and the hypothalamic-pituitary-adrenal (HPA) stress axes, leading to release of neuroendocrine hormones such as epinephrine, adrenocorticotropic hormone (ACTH), and corticosterone into the circulation (Henriquez et al., 2019a; Snow et al., 2018; Kodavanti 2019). These stress hormones have been implicated in a variety of homeostatic processes including leukocyte trafficking and immune surveillance (Ince et al., 2019). In rats, the

pattern of trafficking of circulating leukocytes occurs following treatment with adrenal-derived stress hormones (Miller et al., 1994) which can be recapitulated by restraint stress (Dhabhar et al., 2012; 2014). A 4-hour ozone exposure induces lymphopenia in rats (Miller et al., 2016a, Henriquez et al., 2018a, 2018b; 2019b). Further, the ozone effects are diminished in adrenalectomized rats (Miller et al., 2016b) and by treating animals with stress hormone receptor agonists, these effects reappear (Henriquez et al., 2018b). Ozone has also been shown to increase spleen-derived classical monocytes in the lung (Francis et al., 2017), however, the mechanisms are not well understood.

Stress hormone receptors, such as adrenergic and glucocorticoid, are distributed on a variety of inflammatory cells as well as endothelial cells, which play an important role in rolling, adhesion and extravasation of leukocytes to the tissues where stress is encountered (Padro and Sanders, 2014). Norepinephrine-releasing sympathetic nerve fibers innervate the lymphoid tissues that express adrenergic receptors (Sanders et al., 2001), and β2-adrenergic receptors on B lymphocytes are involved in mediating IgG1 synthesis (Priftis and Chrousos, 2012; Padro and Sanders, 2014). Sympathetic activation has been reported within minutes after air pollution inhalation in rats (Carll et al., 2013), however, its potential contribution to systemic immune response has not been established. Glucocorticoids are potent immunosuppressants and are also involved in leukocyte trafficking (Ince et al., 2019). Glucocorticoids through their transcriptional regulation suppress expression of proinflammatory molecules (Ashwell et al., 2010; Baschant and Tuckermann, 2006) and induce T lymphocyte apoptosis contributing to lymphopenia and immunosuppression (Herold et al., 2006). Lymphocyte apoptosis plays an important role in development, and immune homeostasis and its malfunction is associated with immunodeficiency and autoimmune diseases (Opferman, 2008). Finally, we have shown that ozone-induced lymphopenia is not evident in adrenalectomized rats with diminished circulating epinephrine and corticosterone (Miller et al., 2016b, Henriquez et al., 2018b).

Although ozone-induced lung injury and inflammation are well characterized, no studies have examined the temporal relationship between changes in circulating stress hormones (catecholamines and glucocorticoids) and leukocyte trafficking. To identify initiating event and demonstrate that cytokine changes occur after the release of adrenal-derived stress hormones, it is critical to determine the temporality of events. Adaptive stress response is precisely regulated in duration to prevent excessive injury and initiate repair process. Assessing the dynamics of stress hormones release and innate immune response is critical to understanding the severity of stress inflicted by ozone, how it might relate to recovery from inflammation, and the link between innate and humoral immune effects. The goal of this study was to chronicle the changes in circulating stress hormones and leukocyte trafficking patterns during the course of a 4-hour exposure to ozone to determine precise temporal relationships between stress hormone release and the initiation of leukocyte trafficking, and to delineate the potential connection between inflammation, cytokine changes in the circulation, and stress hormones. Since glucocorticoids are known to induce lymphocyte apoptosis, ozone-induced leukocyte apoptosis was assessed by quantifying live, early- and late-apoptotic, and necrotic cells in blood and immune relevant organs. The changes in leukocyte populations were correlated with circulating inflammatory cytokines and lung markers of inflammation as well as glucocorticoid responsive genes.

2. MATERIALS AND METHODS

2.1. Animals.

Male Wistar Kyoto (WKY) rats (11–12 weeks of age) were purchased from Charles River Laboratories (Raleigh, NC) and pair-housed in polycarbonate cages containing hardwood chip bedding in a controlled environment (temperature 21°C, relative humidity 55–65%, and light/dark 12h cycle) in an animal facility approved by the Association for Assessment and Accreditation of Laboratory Animal Care. Rats were fed Purina 5001 rat chow (Brentwood, MO) and provided tap water, *ad libitum*. Rats were randomized by body weight and allocated to each exposure time group (8/group) prior to study. Experimental protocols were approved by the U.S. EPA's Animal Care and Use Committee. National Institutes of Health guide for the care and use of Laboratory animals (NIH Publications No. 8023) were followed.

2.2. Ozone exposure.

Ozone was used as an environmental stressor which induces lung injury and inflammation. Rats were exposed to filtered air (0.0 ppm), 0.4, or 0.8 ppm ozone for 0.5, 1, 2, or 4 hours (Figure 1). Ozone was generated from oxygen using a silent arc discharge generator (OREC, Phoenix, Arizona) and regulated using mass flow controllers (Coastal Instruments Inc., Burgaw, North Carolina). Targeted ozone concentrations were monitored by photometric analyzers (API Model 400, Teledyne, San Diego, California). Mean temperature, relative humidity, and air flow were monitored throughout the exposure. Exposures occurred over 16 days, 4 days/week for 4 weeks. The chamber ozone concentrations were 0.79 ± 0.01 (mean ± standard deviation of 16 daily averages) for 0.8 ppm chamber and 0.40 ± 0.01 for 0.4 ppm chamber. The chamber average temperature (°F), relative humidity (%) and air flow (liters/minute) were: 71.87 ± 0.70, 44.88 ± 3.02, 263.00 ± 7.57, respectively for air chamber; 72.04 ± 0.45, 42.93 ± 3.36, 240.06 ± 3.48 for 0.4 ppm, respectively ozone chamber; and 72.66 ± 0.32, 42.07 ± 2.89, 262.05 ± 2.41, respectively, for 0.8 ppm ozone chamber.

2.3. Necropsy and tissue samples collection.

To assure rapid and accurate collection of tissues, only six rats were necropsied on a given day immediately following exposure. Rats in each exposure group (0.0, 0.4 or 0.8 ppm) were staggered for necropsies at each time period (0.5, 1, 2, or 4 hours of exposure). Each time point spanned one week of exposures and necropsies (n = 2 animals/group/time point x 4 days/week). Exposure of each duration was also staggered through the 4-hour timeframe (7 am- 11 am) such that necropsy was performed at the same time to avoid diurnal variation in collected parameters. Rats were euthanized within 20 minutes following the end of exposure with an i.p. overdose of sodium pentobarbital (Fatal Plus, Virbac AH, Inc., Fort Worth, TX; >200 mg/kg). Blood samples from the abdominal aorta were collected in one EDTA and one serum separator tube. The EDTA tube was used for assessing hematological parameters and flow cytometry. The serum separator tube was centrifuged (3500 x g for 10 min) and serum samples were stored at −80°C for cytokine quantification. An EDTA blood aliquot was used to perform complete white blood cell count on a Beckman-Coulter AcT blood analyzer (Beckman-Coulter Inc., Fullerton, California). Thymus, spleen and heart were collected and weighed, and thymus and spleen were rapidly processed for flow cytometry analysis. The

left lung was isolated, flash frozen in liquid nitrogen, and stored at 80°C for future gene expression analysis.

2.4. Lung RNA isolation, cDNA synthesis, and quantitative real time PCR (qRT-PCR).

Uniform portions of frozen lung left lobe were cut and weighed (20–30 mg). RNA was extracted using RNeasy mini kits (Qiagen, Valencia, CA) following manufacturer protocols and quantified using a Qubit 2.0 fluorimeter (Thermo Fisher, Waltham, MA). cDNA was synthesized by Qscript Supermix (Quanta Biosciences, Beverly, MA). Primers were designed using Rattus Norvegicus sequences annotated in NCBI and obtained from Integrated DNA Technologies, Inc. (Coralville, IA). The sequences for the primers were: β-actin (*Actb*): f-CAACTGGGACGATATGGAGAAG, r-GTTGGCCTTAGGGTTCAGAG; Chemokine (C-X-C motif) -ligand 2 (*Cxcl2*: f-GCCTCGCTGTCTGAGTTTATC, r- GAGCTGGCCAATGCATATCT; interleukin 6 (*Il6*): f-CTTCACAAGTCGG AGGCTTAAT, r-GCATCATCGCTGTTCATACAATC; heme oxygenase 1 (*Hmox1*): f- CCTGTGTCTTCCTTTGTCTCTC, r- GGGCTCTGTTGCAGGATTT; FK506 binding protein 5, (*Fkbp5*): f- ATCAGCCAAAGTCTCCAGAAC, r- CCCTGCTCAAACCCATAACT; nuclear receptor subfamily 3, group C, member 1 (*Nr3c1*): f- GGGACACGAATGAGGATTGTAA, r- CACACTGCTGGGACTTGATAA; TSC22 domain family protein 3 (*Tsc22d3*): f- CCGAATCATGAACACCGAAATG, r- GCAGAGAAGAGAAGAAGGAGATG.

qRT-PCR was performed using SYBR Green PCR Master Mix (Thermo Fisher, Waltham, MA) and the Applied Biosystems 7900HT Sequence Detection System (Foster City, CA). Relative mRNA expression was calculated using the ΔΔCt method using β-actin as the housekeeping gene and the 30 minute air-exposed group as a control.

2.5. Cytokine and stress hormone quantification in serum and plasma samples.

Serum cytokine concentrations were quantified using the V-PLEX proinflammatory panel 2 (rat) kit following manufacturer's protocol (Mesoscale Discovery Inc., Rockville, MD). Electrochemiluminescence signals were detected using the MESO QuickPlex SQ 120 platform (Mesoscale Discovery Inc., Rockville, MD). Measurement of cytokines was restricted to rats exposed to 0.0 or 0.8 ppm of ozone. For animals in which cytokine levels were below assay detection limits, the values were substituted with the lowest quantified value for the given cytokine in the analysis. Plasma samples from EDTA tubes were used for epinephrine (Rocky Mountain Diagnostics, Colorado Springs, CO) and corticosterone (Arbor Assays, Ann Arbor, MI) analysis. These stress hormones were quantified by ELISA using manufacturer's protocols and the ELISA plates were read on a SpectraMax i3x Multi-Mode Microplate Reader (Molecular Devices, San Jose, CA).

2.6. Tissue and blood cell preparations for flow cytometry.

Thymus and spleen were collected, weighed, immediately cut into four pieces, and submerged in 5 mL of HBSS (without Ca^{+2} and Mg^{+2}) in a 17×100 mm tube. The mix was transferred to a Stomacher® 80 bag and homogenized for 120 seconds in a Stomacher® 80 Biomaster blender (Seward, Bohemia NY). Each cell suspension was transferred back into its tube and residual cells were obtained from the homogenization bag with cold HBSS. The

suspension was then gently mixed and allowed to settle for 5 minutes before transferring the supernatant into a 50 mL conical tube for centrifugation at 500 x g for 5 min. The resulting supernatants were aspirated and the remaining pellet was resuspended in 1 mL of staining buffer (MACS® BSA Stock Solution 1:20 with autoMACS® Rinsing Solution, Miltenyi Biotec, Germany) for cell counting (Z1 Coulter Counter, Coulter, Inc., Miami, FL). A total of 10^7 cells were transferred to a 17×100 mm tube. For spleen, samples were treated with 1X RBC lysis buffer (Thermo Fisher Scientific, Waltham, MA) for 3 minutes, washed twice with 2 mL of staining buffer, and resuspended in 1 mL of staining buffer (Miltenyi Biotec, Germany). For blood, the collected ~3 mL EDTA-blood samples were centrifuged at 3500 x g for 10 min at 4°C. Plasma samples were aliquoted and stored at −80°C for hormone analysis. 200 μL of buffy coat was transferred to a 15 mL conical tube containing 800 μL of cold staining buffer, vortexed and centrifuged (500 x g for 5 min) at room temperature. The supernatant was aspirated and 10 mL of eBioscience 1X RBC lysis buffer (Thermo Fisher Scientific, Waltham, MA) was added to the remaining cell pellet, mixed, and incubated for 10 minutes at room temperature in the dark. The sample was then centrifuged, and the pellet was resuspended in staining buffer. Aliquots of white blood cells, thymocytes and splenocytes were diluted using Isoton and mixed with 0.2 mL saponin to lyse cells. Cell nuclei were counted using a Z1 Coulter Counter (Coulter Inc., Miami, FL).

2.7. Flow cytometry.

The general procedures were performed following previously published methods (DeWitt et al., 2016; Henriquez et al., 2018b; Barnett-Vanes et al. 2016). For each tissue sample 100 μL aliquots per sample were used for treatment with different antibody cocktails (Table 1) that were transferred to 12 × 75mm tubes. Separate aliquots were prepared for fluorescence minus one (FMO) controls to aid in identifying and ensuring accurate gating of negative and positive cell populations. Cells were incubated with 50 μL of color antibody cocktail or 50 μL of isotype control antibody cocktail. In addition to unstained controls, for pooled 100 μL aliquots FMO cocktail or single color antibody solution was added to serve as three different controls (unstained, one color and FMO). Each tube was mixed and incubated for 10 min at 4°C in the dark (Table 1). After incubation with primary antibody, 2 mL of staining buffer was added to each sample, then samples were vortexed and centrifuged (300 x g, 10 min) at room temperature. The supernatant was aspirated and cells were washed twice by centrifugation with 2 mL of serum-free DPBS (centrifuged at 300 x g for 10 min). The cell pellet was resuspended in 1 mL of Fixable eFluor™ 780 viability dye cell staining solution (Thermo Fisher Scientific, Waltham, MA) (1 μL of dye in 1000 μL of serum-free DPBS) and incubated at room temperature for 30 minutes in the dark. Cells were again washed twice by centrifugation, and resuspended in 1 mL of 1X Annexin V binding buffer (Miltenyi Biotec, Somerville, MA, USA), stained with 50 μL of Annexin V-FITC, and incubated at room temperature in the dark for 15 min. Cells were centrifuged, supernatant was aspirated, cells were resuspended in 200 μL of 1X Annexin V binding buffer, and fluorescence-activated cell sorting (FACS) analysis was done within 4 hours.

Data collection, analysis, and quantification were made using LSR II flow cytometer (BD Biosciences, Mississauga, Canada), FACS Diva software (BD Biosciences, Mississauga, Canada) and FlowJo software (TreeStar, Inc., Ashland, Oregon), respectively.

Gating strategies are shown for blood granulocytes and monocytes (Supplementary Materials, Figure 1), blood lymphocytes (Supplementary Materials, Figure 2), thymocytes (Supplementary Materials, Figure 3) and splenocytes (Supplementary Materials, Figure 4). For all blood leukocyte aliquots, whole blood cells were identified by side scatter (SSC-A) and forward scatter (FSC-A). Only singlets were selected and leukocytes ($CD45^+$) identified for all tissues. Strategies for identification of cell subpopulations in both aliquots are described in Table 2. A minimum of 10000 events per sample were counted. For each identified subpopulation, quadrants using viability dye and Annexin V were used to define live, early apoptotic, late apoptotic and necrotic cell populations. Negligible necrotic cells were identified among all cell populations and therefore, the data for these cell populations are not shown.

To assess the ability of dexamethasone to induce apoptosis in isolated white blood cells *in vitro*, these cells were obtained from naïve male WKY rats as shown above, and treated in triplicate with dexamethasone (DEX, dexamethasone sodium phosphate, Henry Schein, Dublin, OH) at three dose levels (0.0 mM, 0.1 mM and 1.0 mM) for 2 hours. Annexin V-FITC was then added to cells to determine the levels of apoptotic cells while unstained cells were used as negative control. Lymphocytes and monocytes were identified by side-scatter and forward-scatter, and the percentage of Annexin V+ cells were determined (Supplementary Materials Figure 5). Dexamethasone at these concentrations moderately increased the number of annexin V+ total cells, suggesting some effect on circulating lymphocytes and monocytes.

2.8. Statistics.

For thymus and spleen subpopulations, absolute cell numbers were calculated using relative percentage of each cell type and total cell number. For blood, the results were reported as cells/ml. For all other endpoints, differences between air and each ozone concentration at each time of exposure were analyzed using one-way non-parametric analysis of variance (ANOVA, Kruskal-Wallis test). Since the non-normally distributed data were derived through multiple calculations, a non-parametric test was used to avoid further transformation. Multiple comparisons were done using Dunn's multiple comparison test, and values were considered significant at $P \leq 0.05$. For ease of comparison, only significant ozone exposure effects are shown in the tables and figures since each time point involved an independent control group. Graphs and tables show means and SEM (n=6–8 animals/group). Although 8 rats per group were planned in the experimental design, as few as 6 rats were analyzed in some groups, since ~10% Wistar Kyoto rats exhibit spontaneous cardiac hypertrophy, which causes no pathogenic cardiac functional alterations but is often associated with lung inflammation (Shannahan et al., 2010). Therefore, the data coming from rats with 20% or greater heart weight relative to other rats were not considered to eliminate any baseline health-related changes in biological parameters of interest. For the summary diagram (Figure 10), results were expressed as % of change from 0.0 ppm ozone (air controls) for each time of exposure. GraphPad Prism 8 (version 8.4.2) was used for statistical analysis and graph design.

3. RESULTS

3.1. Time-dependent ozone-induced increases in circulating stress hormones and pulmonary gene expression.

During the 4-hour ozone exposure, there were no major exposure-related changes in body weights or hematological parameters including hematocrit and blood platelets (Supplementary Materials, Figure 6). Since injury and inflammation might not be evident in the lung prior to 4 hours of exposure, lung gene expression was examined for markers of inflammation. Markers downstream of glucocorticoid signaling were also analyzed to understand their temporal activation in relation to changes in circulating stress hormones. Circulating epinephrine and corticosterone were increased as early as 1 hour of 0.8 ppm ozone exposure and continued to be higher after 2 and 4 hours (Table 3). Although not significant, it is noteworthy that the air-exposed animals showed a small increase in corticosterone at 1 hour time point suggesting that handling and placing animals in wire-mesh cages could result in a transient rise in stress hormone levels. Since the small rise in corticosterone occurred only at 1-hour time point in controls even though the day-light time animals were placed in wire-mesh cages varied between 7 am to 10:30 am, it is likely that handling and placing animals in exposure chambers caused a transient stress response.

Cxcl2, also known as macrophage inflammatory protein-2 (*Mip-2*), is involved in neutrophilic inflammatory response and was increased only after 4 hours of exposure to 0.8 ppm ozone in the lung (Figure 2A). However, small increases in lung *Il6* expression began to occur at 2 hours and markedly increased after 4 hours of exposure to 0.8 ppm ozone (Figure 2B). *Hmox1*, another marker for oxidative stress, was only increased following 4 hours of 0.8 ppm ozone exposure (Figure 2C). These data suggest that during ozone exposure, upregulation of pulmonary inflammatory gene expression occurs after the observed increases in circulating stress hormones. To assess if increased circulating stress hormones change glucocorticoid responsive genes, their expression was assessed in the lung. The gene for glucocorticoid receptor (*Nrc31*) was significantly increased following 4 hours of exposure to 0.8 ppm ozone, suggesting a glucocorticoid response in the lung (Figure 2D). The glucocorticoid responsive gene, *Fkbp5*, increased nearly 5-fold at 2 hours of exposure to 0.8 ppm ozone and was further increased at 4 hours (Figure 2E). At the 0.4 ppm exposure concentration, *Fkpb5* was upregulated after 4 hours. Similarly, *Tsc22d3*, another glucocorticoid responsive gene with anti-inflammatory activity (Bereshchenko et al. 2019), increased its expression after 2 hours point and was further increased at 4 hours of 0.8 ppm ozone exposure (Figure 2F).

3.2. Temporal changes in circulating cytokines during ozone exposure

To determine if changes in circulating stress hormones and inflammatory endpoints in the lung were associated with release of cytokine proteins in the circulation that have been implicated in air pollution health effects, a battery of cytokines were analyzed in serum samples from air and 0.8 ppm ozone-exposed rats (Figure 3). Small increases were noted in circulating IL-6 after 4 hours of ozone exposure. In contrast, levels of TNF-α were decreased at 2 and 4 hours of ozone exposure (Figure 3A, B). Serum IFN-γ did not change and the levels of IL-1β were slightly increased at 4 hours of ozone exposure (Figure 3C,

D). Likewise, serum IL-4 and IL-5 increased slightly but significantly at 4 hours of ozone exposure (Figure 3E, F). Serum levels of the neutrophil chemoattractant KC-GRO (CXCL1) were significantly reduced at both 1 hour and 4 hours in ozone-exposed rats (Figure 3G). The levels of anti-inflammatory cytokines IL-10 and IL-13 were slightly increased in ozone-exposed animals at 1 hour and 4 hour time points (Figure 3H, I). These data demonstrate modest changes in many circulating cytokines after 4 hours, with decreases in TNF-α and KC-GRO. The genes for both these cytokines are known to be inhibited by steroidal drugs (Steer et al., 2000; Chen et al., 2018).

3.3. Dynamic changes in circulating granulocytes and monocytes over 4-hour ozone exposure

By assessing different circulating leukocyte populations, the redistribution of leukocytes and the specificity with the type of cells in relation to stress hormones were determined at various times after ozone exposure. . Circulating $CD45^+$ total granulocytes were increased after 30 minutes at 0.8 and 0.4 ppm ozone exposure; however, their concentration declined at 2 and 4 hours of 0.8 ppm ozone exposure (Figure 4A). After 4 hours of air or ozone exposure, 17–25% of all granulocytes were early apoptotic, and almost no late apoptotic cells were present suggesting no influence of ozone. A 30% decrease in circulating monocytes occurred at 4 hours after 0.8 ppm of ozone exposure, however this was statistically insignificant (Figure 4B). There was no ozone effect on monocyte apoptosis.

When monocytes were labelled for surface markers to separate classical (inflammatory) and non-classical (anti-inflammatory/repair) phenotypes, classical monocytes decreased in the circulation at 2 hours of 0.8 ppm of ozone exposure with a further decline by 4 hours (Figure 5A). Although not significant, the same trend was observed at 0.4 ppm ozone. At 4 hours, about 24–27% of classical monocytes displayed an early apoptotic phenotype regardless of ozone exposure, and no cells undergoing apoptosis were identified (Figure 5A). The ozone-induced decline in non-classical monocytes was not significant (Figure 5B). At 4 hours, only about 9% of non-classical monocytes expressed early apoptosis cell surface markers regardless of exposure (Figure 5B). Ozone exposure did not significantly change the percentage of apoptotic cells for classical or non-classical monocytes (Figure 5A,B).

3.4. Ozone-induced decline in circulating lymphocyte populations at different times over a 4-hour exposure period

Total circulating lymphocytes declined as early as 1 hour of ozone exposure and lymphocytes then progressively dropped over a 4 hour exposure to 0.8 ppm ozone (Figure 6). Circulating lymphocytes did not significantly decrease over 4 hours of exposure to 0.4 ppm ozone. The data obtained using flow cytometry for decline in circulating lymphocytes correlated well with data obtained using a conventional hematological analyzer, verifying these ozone-induced changes (Supplementary Materials, Figure 7A, B). As expected, the lymphocyte changes were similar to those observed for white blood cells since in rats the majority of white blood cells are lymphocytes (Supplementary Materials, Figure 7C, Reich and Dunning, 1943). After 4 hours of air or 0.8 ppm ozone exposure about 11–14% lymphocytes were in the early apoptosis stage, while 2–4% were in the late apoptosis stage.

Ozone-exposed animals had 4% late apoptotic cells relative to air with 2% apoptotic cells, but this change was not significant (Figure 6).

To determine the types of lymphocytes most affected by ozone exposure in the circulation, B lymphocytes (CD45R+) involved in adaptive humoral immunity and T lymphocytes (CD3+) involved in cell-mediated immunity were identified (Figure 7). Ozone exposure at 0.8 ppm led to a marked time-dependent drop in circulating B lymphocytes starting at 1 hour and progressing to below 50% of air control by 4 hours (Figure 7A). B lymphocytes also dropped in the group exposed to 0.4 ppm ozone but only at the 4 hour time point. The proportion of early apoptotic cells ranged from 16–20% with 2–4% in late apoptotic stage regardless of air or ozone exposure. Circulating T lymphocytes dropped after 0.8 ppm ozone exposure in a time-related manner but to a lesser degree (~25%) when compared with B lymphocytes. Only about 8% of cells were found to be in the early apoptotic stage and 2–4% in late apoptotic stage regardless of exposure. Ozone did not induce significant changes in apoptotic cell subpopulations (Figure 7B).

T lymphocytes were further separated as CD4+ T-helper versus CD8+ T-cytotoxic cells to determine ozone effects on each subtype. T-helper CD4+CD8− cells decreased after 0.8 ppm ozone starting at 1 hour; however, this decrease was not significant (Figure 8A). The proportion of early apoptotic cells was 7–8% at the 4-hour time point and was unaffected by ozone exposure. Cytotoxic CD4-CD8+ T lymphocytes decreased significantly after 4 hours of exposure to 0.8 ppm ozone (Figure 8B). At the 4 hour time point, the proportion of early apoptotic cells remained similar in all exposure groups (7–9%). Both CD4+CD8+ and CD4-CD8− were relatively low in abundance compared with either T-helper or T-cytotoxic cells and large time-related variations were noted regardless of air or ozone exposure. This could be due to few number of cells and also different week of assessment for each timepoint (Figure 9). A small but significant drop in CD4+CD8+ cells was observed at 4 hours of exposure to 0.8 ppm ozone (Figure 9A) with 10–12% cells in early apoptotic stage and 7–11% in late apoptotic stage in both air and ozone exposure group. T lymphocytes expressing neither surface marker (CD4-CD8−) also decreased after 0.8 ppm ozone exposure, reaching significance by the 4-hour time point. It is noteworthy that unlike other cell types and regardless of air or ozone exposure, a large proportion of these cells expressed early apoptotic or late apoptotic phenotypes (24–28% early apoptotic; 23–31% late apoptotic) (Figure 9).

For all types of circulating white blood cells, the relative percentage change from matching air controls after 0.4 and 0.8 ppm of ozone exposure is summarized in Figure 10. The increase in blood granulocytes at 30 minutes after ozone exposure may reflect their early release from bone marrow followed by their extravasation to lung microvasculature (Figure 10A). It was interesting to note that the major share of monocytes in the blood in ozone-exposed rats belonged to the classical phenotype, and no significant ozone-related changes were noted in non-classical macrophages (Figure 10B). Lymphocytes were reduced at 4 hours of ozone exposure (Figure 9A). This was reflected in ozone concentration-related drops in circulating B and T lymphocytes (Figure 10C); the drop in B lymphocytes being more pronounced than T. Among T helper and cytotoxic lymphocytes, the ozone-induced decrease was significant for cytotoxic (CD8+) T cells (Figure 10D).

3.5. Thymus and spleen lymphocyte populations and ozone effects

In order to understand the source of lymphocytes and potential acute ozone-induced alterations in the thymus where T lymphocytes mature and the spleen through which both T and B lymphocytes transit, the number of lymphocytes in these organs were determined. There were small increases in spleen but not thymus weights for the group exposed to 0.8 ppm of ozone for 2 hours (Supplementary Materials, Figure 8A, B). The numbers of thymocytes and splenocytes quantified in thymus and spleen, respectively, did not change consistently with ozone exposure (Supplementary Materials, Figure 8C, D). It should be noted that there were time-related differences in the lymphocyte populations from thymus and spleen as observed with circulating white blood cells which could relate to experimental variation. There were no consistent ozone exposure-related changes in thymus or spleen total and individual lymphocyte subpopulations (Figure 11A–E) within a short time span of 4 hour ozone exposure.

4. DISCUSSION

The contribution of the neuroendocrine system to air pollution health effects is underappreciated. It is presumed that cytokines released systemically from injured lung after inhalation of air pollution are responsible for extrapulmonary effects. Recent studies have shown that a single exposure to ozone, a prototypical air pollutant, is associated with the activation of SAM and HPA axes (Kodavanti 2016; Snow et al., 2018), which promotes the release of epinephrine and corticosterone into the circulation. These hormones play a role in pulmonary and systemic effects of ozone (Miller et al., 2016b). Further, ozone-induced lung inflammation and lymphopenia are diminished in adrenalectomized rats, and that the effect of adrenalectomy can be reversed by treating animals with agonists of adrenergic plus glucocorticoid receptors (Henriquez et al., 2018). Circulating adrenal-derived stress hormones are known to mediate leukocyte trafficking by regulating their egress from bone marrow and lymphoid organs, and extravasation to the site of stress (Ince et al., 2019). It was postulated that ozone exposure will induce changes in the pool of circulating granulocytes, monocytes and lymphocytes in a time-related manner, together with lung inflammatory changes and that this response will be preceded by increases in circulating epinephrine and corticosterone. The data show that ozone exposure leads to dynamic changes in leukocyte trafficking through blood and induces lung markers of inflammation that are preceded by increases in circulating stress hormones. However, apoptosis of lymphocytes, known to occur with glucocorticoid treatment (Herold et al., 2006), was not evident in the experimental time frame in the circulation, thymus or spleen as a result of ozone exposure. This temporal assessment of ozone effects allowed establishment of the relationship between stress hormones and kinetics of changes in different immune cells, which is critical in understanding how the stress-induced innate immune response is shaped and how it is linked to humoral immune changes. There are no prior studies linking the dynamic aspects of stress and the innate immune response during ozone exposure.

Egress from bone marrow to blood and extravasation of immune cells has been shown to be regulated by adrenal-derived stress hormones, namely epinephrine and corticosterone (Dhabhar et al., 2012; Dhabhar 2014). Significant increases in both circulating stress

hormones starting at 1 hour of ozone exposure were followed by a marked increase in lung glucocorticoid and inflammatory cytokine gene expression at 2 and 4 hours of exposure, respectively. With increasing stress hormones, a rapid increase was noted in total granulocytes at 30 minutes followed by a general decline starting at 1 hour into ozone exposure, which is likely reflective of the egress of marginated neutrophils from the bone marrow followed by their margination to the lung. A time-related decline in classical monocytes over 4 hours of ozone exposure also follows increases in circulating epinephrine and corticosterone. There were also significant declines in total, T-cytotoxic, and B lymphocytes in blood, at 2 and 4 hours of ozone exposure, but no significant changes were noted in thymus or spleen lymphocyte populations or increase in apoptotic lymphocytes. These data suggest the initial margination of circulating monocytes and granulocytes likely to the lung, which may follow the changes in lymphoid organs that have been noted with longer ozone exposures (Dziedzic and White, 1986; Francis et al., 2017). The kinetic relationship between adrenal-derived hormones and the trafficking of blood leukocytes in response to ozone exposure may explain the sequelae of events that results in lung inflammation. Early increases in stress hormones followed by later minor changes in circulating cytokines in this study may suggest that systemic air pollution effects might not involve circulating cytokines.

The rapid increases in circulating adrenal-derived hormones point to the role of neural activation (Henriquez et al., 2019b). The effects of increased circulating adrenal-derived stress hormones, especially corticosterone, on lung gene expression is reflective of increased glucocorticoid signaling. FKBP5 encodes for a co-chaperone of hsp90 which regulates glucocorticoid receptor (GR) sensitivity (Wiechmann et al., 2019) and its associated downstream gene (*Tsc22d3*) is involved in suppressing the transcription of proinflammatory genes (Bereshchenko et al., 2019). Despite ozone-induced increases in the expression of glucocorticoid responsive gene targets in the lung, the increases of *Il6* and other proinflammatory genes, such as Cxcl2 was not inhibited suggesting a complex interaction of multiple mechanisms. Proinflammatory effects of glucocorticoids have been shown in some experimental conditions (Horowitz et al., 2020). Moreover, the concurrent increases in epinephrine may stimulate inflammatory gene expression through activation of β2 adrenergic receptors on macrophages (Chiarella et al., 2014) and lung epithelial cells (Ritchie et al., 2018) resulting in inflammation in the lung (Henriquez et al., 2019b).

Circulating bioactive mediators, such as cytokines and oxidation byproducts released from the lung have been proposed to mediate systemic and peripheral effects of air pollutants; however, no specific effector molecules have been consistently verified. The evidence for increases in circulating cytokines following exposure to air pollutants is inconsistent. The modest increases in circulating IL-6 and other cytokines at 4 hours of ozone and decreases in TNF-α and KC-GRO suggest that pulmonary-derived cytokines are not likely responsible for peripheral effects of ozone in this acute scenario. However, sustained increases in circulating cytokines in chronic illnesses have been proposed to contribute to disease pathogenesis (Hughes et al., 2020). The depletion of circulating TNF-α may relate to inhibition by circulating glucocorticoids (Steer et al., 2000) as the levels of corticosterone were increased in a time and concentration-dependent manner in ozone-exposed rats, which was followed by depletion of lymphocytes and these cytokines. Ozone exposure increases

lipid metabolites and acute phase proteins in the circulation along with increases in adrenal-derived stress hormones (Bass et al., 2013; Miller et al., 2015, 2016a). Stress hormones appear to play a key role in mediating ozone-induced lung effects, since depletion of circulating stress hormones diminishes all ozone effects on the lung and in the periphery including lymphopenia (Miller et al, 2015; Henriquez et al, 2018b; 2019a). Based on this evidence, it could be suggested that local lung injury and cytokine expression after acute air pollution exposure may occur through interaction of the activities of stress hormone receptors, and local cellular changes induced by pollutants.

The early increase in epinephrine was likely triggered by ozone-induced sympathetic nerve activation (Hajat et al., 2019), which could have accounted for the rapid increase at 30 minutes of exposure in circulating total granulocytes, likely neutrophils that are readily available for release from lymphoid organs, such as blood vessels and bone marrow. Inhalation of particulate matter has been shown to increase circulating band cells which are premature neutrophils (van Eeden et al., 2005, Ao et al., 2020). The rapid rise in circulating granulocytes may suggest that their mobilization is likely from tissues innervated by sympathetic nerves, such as the blood vessels and bone marrow. In mice during circadian oscillation, norepinephrine-mediated paracrine activation of adrenergic receptors was shown to downregulate the key retention factor CXCl12 leading to mobilization of hematopoietic progenitor cells (Méndez-Ferrer et al., 2008). The concentrations of catecholamines and glucocorticoids at the site of action were shown to be critically important in margination of leukocytes (Ince et al., 2019). Dexamethasone has been shown to increase de-margination of granulocytes and also affect the expression of surface receptors on leukocytes that lead to their maturation and egress (Fay et al., 2016). The initial increase and then reduction of granulocytes is consistent with the nature of pulmonary inflammation characterized by neutrophilia in the lungs hours after an acute ozone exposure (Kodavanti et al., 2015; Henriquez et al., 2019b). The depletion of proinflammatory classical monocytes in the circulation after ozone exposure is consistent with the observation that these cells are extravasated to the lung (Francis et al., 2017).

By regulating lymphocyte differentiation, migration and apoptosis, glucocorticoids maintain homeostatic control in multiple lymphoid tissue and blood compartments. One of the mechanisms by which glucocorticoids play a regulatory role in lymphocyte homeostasis during steady state or stress is through their anti-inflammatory effects, and by inducing apoptosis of both B and T lymphocytes in lymphoid organs (Boldizsar et al., 2010; Kfir-Erenfeld and Yefenof, 2014; Krüger and Mooren, 2014; Evangelisti et al., 2018). However, we noted that although circulating lymphocytes were depleted by ozone in the blood, only a modest increase occurred in apoptotic cells despite sustained increases in circulating corticosterone over 4 hours. Moreover, circulating leukocytes from naïve rats incubated with dexamethasone *in vitro* had only moderately increased apoptotic (Annexin V+) cells (Supplementary Materials, Figure 5). It is likely that the pro-apoptotic effect of glucocorticoids requires a much greater concentration than that occurred following ozone exposure in healthy rats and that other stress mechanisms might also be involved. In this rat model, the margination of lymphocytes to pulmonary vasculature may be responsible for observed ozone-induced lymphopenia. Although we were not able to consistently demonstrate the increased presence of lymphocytes in the lung lavage fluid

after ozone exposure, the rats pretreated with β-adrenergic and glucocorticoid receptor blockers and exposed to ozone had significant depletion of these cells relative to non-treated ozone-exposed rats (Henriquez et al., 2018a), suggesting their potential margination to the interstitial lung compartment and/or lung-associated lymphoid tissues.

To further understand the relationship between the timing of stress hormone release and leukocyte redistribution, and their potential contribution to ozone-induced inflammatory responses, temporal changes were characterized in B and T lymphocyte subpopulations. Rapid declines in circulating B and T lymphocytes after ozone exposure suggests that the effect of ozone is occuring in all lymphocyte populations; with B cells more severely depleted than T cells at the 4 hour time point (60–70% vs. ~30%, respectively). B cells play a role in humoral immunity by antibody production upon recognition of antigen. The depletion of these cells in the circulation may relate to their redistribution to lung or lung-associated or other lymphatic tissues. It has been shown that ozone exposure in a mouse model increases T but not B lymphocytes in lung interstitial spaces (Bleavins and Dziedzic, 1990). Increased presence of T lymphocytes in the lavage fluid after ozone exposure was also noted in humans (Holz et al., 2001). Given the role of T lymphocytes in cell-mediated immunity, they might contribute to ozone-induced lung injury and inflammatory response.

A variety of cell surface markers can distinguish T lymphocyte phenotypes with differential functional roles (Kinoshita and Hato, 2001). CD4+ T-helper cells enhance the function of B cells to produce antibody while CD8+ T cells are cytotoxic to target cells (Koretzky, 2010). Decreases in CD4 and CD8 mixed cell populations after ozone exposure is consistent with their migration to the lung where ozone-induced cellular changes are occuring likely in response to stress-induced increases in circulating stress hormones. Both epinephrine and corticosterone are known to affect T cell maturation in the thymus and their migration to sites of injury (Savino et al., 2016). Ozone-induced decreases, especially in circulating cytotoxic (CD8+) T cells suggest their tissue margination at early time points and contribution to lung injury. Overall, the ozone induced innate immune response also involves changes in adaptive immune cells.

In this study, no major ozone-induced changes were noted in thymocyte or splenocyte cell populations or organ weights despite observed decreases in circulating lymphocytes. Stress-induced release of glucocorticoids has been shown to cause thymic involution (Bauer et al., 2015). Ozone exposure has long been shown to induce thymic atrophy (Dziedzic and White, 1986) and other thymocyte effects (Feng et al., 2006; Li and Richters, 1991) often without effect on thymus weight (Fujimaki H, Kawagoe, 1990). It is likely that major weight or cellular changes in the thymus or spleen may require longer exposures or higher ozone concentrations. Long-term immunological consequences of ozone may involve thymic atrophy and humoral immune changes.

This temporal assessment addresses how the inflammatory events are initiated within minutes through the activation of neuroendocrine system during the first encounter of ozone, which leads to migration of innate immune cells to the lung in following hours. Despite the lung inflammatory response being maximum on the next day, the hormonal changes and other effects directly linked to neuroendocrine activation, such as hyperglycemia, are

reversible (Kodavanti et al., 2015; Miller et al., 2015), suggesting the plasticity of the response that is involved in lung inflammation and injury. Upon repeated daily ozone exposure, ozone-induced lung injury and inflammation are still apparent in the second day but nearly absent on the third day despite recurrent ozone exposure (Miller et al., 2016b). This evidence suggests that the adaptation to ozone is dynamic and the chronicity of effects likely depend on the host susceptibility and the functionality of the neuroendocrine system.

Although bone marrow and lung tissue were assessed for presence of different leukocytes, the data did not provide consistent findings with high variability in the yield between replicates. Moreover, because of the limitation of the availability of desired antibodies for rats, additional target cell subpopulations were not quantified in this study. The ozone concentrations used are several folds higher than what may be encountered environmentally (U.S. EPA, 2020), however, are comparable to human clinical studies. This is based on the evidence that humans inhaling ozone during intermittent exercise retain 4–5 times greater ozone dose in the lung lining fluid compared to rats exposed during rest and inactivity period (Hatch et al., 2013). Also, this study did not address the potential consequences of stress response after chronic ozone exposure. Finally, only male rats were included in this study.

5. Conclusion.

In conclusion, this study demonstrates temporal changes in circulating leukocyte trafficking during a 4-hour ozone exposure that follows early increases in adrenal-derived stress hormones, but not circulating cytokines. The increased expression of glucocorticoid responsive gene markers and inflammatory cytokines in the lung also follows stress hormone increases. After a rapid increase of granulocytes in the circulation at 30 minutes of ozone exposure, there is a decline over 4 hours. A general decline in classical monocytes and B as well as T lymphocytes is also preceded by increases in circulating stress hormones. These changes do not involve increases in apoptotic monocytes or lymphocytes. The decline in classical monocytes and T lymphocytes in blood is consistent with their reported increase in the lung after ozone exposure (Francis et al., 2017; Bleavins and Dziedzic, 1990). Thus, the temporal changes in circulating stress hormones, granulocytes, monocytes, and B and T lymphocytes during a 4-hour exposure period suggests that ozone-induced increases in epinephrine and corticosterone may mediate redistribution of immune cells to the lung.

Supplementary Material

Refer to Web version on PubMed Central for supplementary material.

Acknowledgements:

The authors thank Drs. Ian Gilmour and Aimen Farraj of the US EPA for their critical review of the manuscript; and Dr. Kimberly Gowdy of the Ohio State University for her expert assistance in the study and review of the manuscript. We acknowledge the help of Dr. Mark Higuchi and Mr. Abdul Malek Khan of the US EPA for ozone inhalation exposures. A.R.H. was supported in part by Fulbright (Becas Chile, CONICYT; IIE-15120279).

Funding:

This project was supported by the US EPA's Intramural Research Program and in past by appointments (AHC, CC, DA, CM) to Research Participation Program at the PIHTD, CPHEA, US EPA, administered by the Oak Ridge Institute for Science and Education through an interagency agreement between the U.S. Department of Energy.

6. References

Ao T, Kikuta J, Sudo T, Uchida Y, Kobayashi K, Ishii M 2020. Local sympathetic neurons promote neutrophil egress from the bone marrow at the onset of acute inflammation [published online ahead of print, 2020 Apr 10]. Int Immunol. dxaa025. doi:10.1093/intimm/dxaa025

Ashwell JD, Lu FW, Vacchio MS 2000. Glucocorticoids in T cell development and function*. Annu Rev Immunol. 18:309–345. doi:10.1146/annurev.immunol.18.1.309 [PubMed: 10837061]

Barnett-Vanes A, Sharrock A, Birrell MA, Rankin S 2016. A Single 9-Colour Flow Cytometric Method to Characterise Major Leukocyte Populations in the Rat: Validation in a Model of LPS-Induced Pulmonary Inflammation. PLoS One. 11(1):e0142520. Published 2016 Jan 14. doi:10.1371/journal.pone.0142520 [PubMed: 26764486]

Baschant U, Tuckermann J 2010. The role of the glucocorticoid receptor in inflammation and immunity. J Steroid Biochem Mol Biol. 120(2–3):69–75. doi:10.1016/j.jsbmb.2010.03.058 [PubMed: 20346397]

Bass V, Gordon CJ, Jarema KA MacPhail RC, Cascio WE, Phillips PM, et al. 2013. Ozone induces glucose intolerance and systemic metabolic effects in young and aged Brown Norway rats. Toxicol Appl Pharmacol.273(3):551–560. doi:10.1016/j.taap.2013.09.029 [PubMed: 24103449]

Bauer ME, Wieck A, Petersen LE, Baptista TS 2015. Neuroendocrine and viral correlates of premature immunosenescence. Ann N Y Acad Sci. 1351:11–21. doi: 10.1111/nyas.12786. Epub 2015 May 5. PMID: 25943573. [PubMed: 25943573]

Bereshchenko O, Migliorati G, Bruscoli S, Riccardi C 2019. Glucocorticoid-Induced Leucine Zipper: A Novel Anti-inflammatory Molecule. Front Pharmacol. 10:308. Published 2019 Mar 27. doi:10.3389/fphar.2019.00308 [PubMed: 30971930]

Bleavins MR, Dziedzic D 1990. An immunofluorescence study of T and B lymphocytes in ozone-induced pulmonary lesions in the mouse. Toxicol Appl Pharmacol. 105(1):93–102. doi:10.1016/0041-008x(90)90361-w [PubMed: 2203188]

Boldizsar F, Talaber G, Szabo M, et al. 2010. Emerging pathways of non-genomic glucocorticoid (GC) signalling in T cells. Immunobiology. 215(7):521–526. doi:10.1016/j.imbio.2009.10.003 [PubMed: 19906460]

Carll AP, Hazari MS, Perez CM, et al. 2010. An autonomic link between inhaled diesel exhaust and impaired cardiac performance: insight from treadmill and dobutamine challenges in heart failure-prone rats. Toxicol Sci. 135(2):425–436.

Chen S, Zaifman J, Kulkarni JA, Zhigaltsev IV, Tam YK, Ciufolini MA,et al. 2018. Dexamethasone prodrugs as potent suppressors of the immunostimulatory effects of lipid nanoparticle formulations of nucleic acids. J Control Release. 286:46–54. doi:10.1016/j.jconrel.2018.07.026 [PubMed: 30026080]

Chiarella SE, Soberanesm S, Urich D, Morales-Nebreda L, Nigdelioglu R, Green D, et al. 2014.β_2-Adrenergic agonists augment air pollution-induced IL-6 release and thrombosis. J Clin Invest. 124:2935–2946. [PubMed: 24865431]

DeWitt JC, Germolec DR, Luebke RW, Johnson VJ 2016. Associating Changes in the Immune System with Clinical Diseases for Interpretation in Risk Assessment. Curr Protoc Toxicol. 67(1):18.1.1–18.1.22. doi: 10.1002/0471140856.tx1801s67. PMID: 26828330; PMCID: PMC4780336.

Dhabhar FS, Malarkey WB, Neri E, McEwen BS 2012. Stress-induced redistribution of immune cells--from barracks to boulevards to battlefields: a tale of three hormones--Curt Richter Award winner. Psychoneuroendocrinology. 37(9):1345–1368. doi:10.1016/j.psyneuen.2012.05.008 [PubMed: 22727761]

Dhabhar FS 2014. Effects of stress on immune function: the good, the bad, and the beautiful. Immunol Res. 58(2–3):193–210. doi:10.1007/s12026-014-8517-0 [PubMed: 24798553]

Dziedzic D, White HJ 1986. Thymus and pulmonary lymph node response to acute and subchronic ozone inhalation in the mouse. Environ Res. 41(2):598–609. doi: 10.1016/s0013-9351(86)80154-2. PMID: 3780655. [PubMed: 3780655]

Evangelisti C, Cappellini A, Oliveira M, Fragoso R, Barata JT, Bertaina A et al. 2018. Phosphatidylinositol 3-kinase inhibition potentiates glucocorticoid response in B-cell acute lymphoblastic leukemia. J Cell Physiol.233(3):1796–1811. doi:10.1002/jcp.26135 [PubMed: 28777460]

Fay ME, Myers DR, Kumar A, Turbyfield CT, Byler R, Crawford K, et al. 2016. Cellular softening mediates leukocyte demargination and trafficking, thereby increasing clinical blood counts. Proc Natl Acad Sci U S A. 113(8):1987–1992. doi:10.1073/pnas.1508920113 [PubMed: 26858400]

Feng R, He W, Ochi H, Castranova V 2006. Ozone exposure impairs antigen-specific immunity but activates IL-7-induced proliferation of CD4-CD8− thymocytes in BALB/c mice. J Toxicol Environ Health A. 69(16):1511–26. doi: 10.1080/15287390500468696. PMID: 16854782. [PubMed: 16854782]

Francis M, Groves AM, Sun R, Cervelli JA, Choi H, Laskin JD,et al. 2017. Editor's Highlight: CCR2 Regulates Inflammatory Cell Accumulation in the Lung and Tissue Injury following Ozone Exposure. Toxicol Sci. 155(2):474–484. doi:10.1093/toxsci/kfw226 [PubMed: 27837169]

Fujimaki H, Kawagoe A 1990. Enhanced antibody production in W/Wv mice exposed to ozone. Toxicol Lett. 53(3):343–7. doi: 10.1016/0378-4274(90)90239-i. PMID: 2237941. [PubMed: 2237941]

Gasteiger G, D'Osualdo A, Schubert DA, Weber A, Bruscia EM, Hartl D 2017. Cellular Innate Immunity: An Old Game with New Players. J Innate Immun. 9:111–125. doi: 10.1159/000453397 [PubMed: 28006777]

Hajat A, Diez Roux AV, Castro-Diehl C, Cosselman K, Golden SH, Hazlehurst MF, et al. 2019. The Association between Long-Term Air Pollution and Urinary Catecholamines: Evidence from the Multi-Ethnic Study of Atherosclerosis. Environ Health Perspect. 127(5):57007. doi:10.1289/EHP3286 [PubMed: 31095432]

Hatch GE, McKee J, Brown J, et al. 2013. Biomarkers of Dose and Effect of Inhaled Ozone in Resting versus Exercising Human Subjects: Comparison with Resting Rats. Biomark Insights. 8:53–67. PMID: 23761957; PMCID: PMC3663491. [PubMed: 23761957]

Henriquez A, House J, Miller DB, et al. 2017. Adrenal-derived stress hormones modulate ozone-induced lung injury and inflammation. Toxicol Appl Pharmacol. 329:249–258. doi:10.1016/j.taap.2017.06.009 [PubMed: 28623178]

Henriquez AR, Snow SJ, Schladweiler MC, Miller CN, Dye JA, Ledbetter AD, et al. 2018a. Adrenergic and glucocorticoid receptor antagonists reduce ozone-induced lung injury and inflammation. Toxicol Appl Pharmacol. 339:161–171. doi:10.1016/j.taap.2017.12.006 [PubMed: 29247675]

Henriquez AR, Snow SJ, Schladweiler MC, Miller CN, Dye JA, Ledbetter AD, et al. 2018b. Beta-2 Adrenergic and Glucocorticoid Receptor Agonists Modulate Ozone-Induced Pulmonary Protein Leakage and Inflammation in Healthy and Adrenalectomized Rats. Toxicol Sci. 166(2):288–305. doi:10.1093/toxsci/kfy198 [PubMed: 30379318]

Henriquez AR, House JS, Snow SJ, Miller CN, Schladweiler MC, Fisher A, et al. 2019a. Ozone-induced dysregulation of neuroendocrine axes requires adrenal-derived stress hormones [published online ahead of print, 2019a Aug 9]. Toxicol Sci.;kfz182. doi:10.1093/toxsci/kfz182 [PubMed: 31397875]

Henriquez AR, Snow SJ, Schladweiler MC, Miller CN, Dye JA, Ledbetter AD, et al. 2019. Exacerbation of ozone-induced pulmonary and systemic effects by β_2-adrenergic and/or glucocorticoid receptor agonist/s. Sci Rep. 2019b;9(1):17925. doi:10.1038/s41598-019-54269-w [PubMed: 31784596]

Herold MJ, McPherson KG, Reichardt HM 2006. Glucocorticoids in T cell apoptosis and function. Cell Mol Life Sci. 63(1):60–72. doi:10.1007/s00018-005-5390-y [PubMed: 16314919]

Holz O, Böttcher M, Timm P, Koschyk S, Abel G, Gercken G, et al. 2001. Flow cytometric analysis of lymphocyte subpopulations in bronchoalveolar lavage fluid after repeated ozone exposure. Int Arch Occup Environ Health. 74(4):242–248. doi:10.1007/s004200000216 [PubMed: 11401015]

Horowitz MA, Cattaneo A, Cattane N, Lopizzo N, Tojo L, Bakunina N, et al. 2020. Glucocorticoids prime the inflammatory response of human hippocampal cells through upregulation of inflammatory pathways [published online ahead of print, 2020 Mar 16]. Brain Behav Immun. S0889–1591(19)31401–1. doi:10.1016/j.bbi.2020.03.012

Hughes MJ, McGettrick HM, Sapey E 2020. Shared mechanisms of multimorbidity in COPD, atherosclerosis and type-2 diabetes: the neutrophil as a potential inflammatory target. Eur Respir Rev. 29(155):190102. doi: 10.1183/16000617.0102-2019. PMID: 32198215. [PubMed: 32198215]

Ince LM, Weber J, Scheiermann C 2019. Control of Leukocyte Trafficking by Stress-Associated Hormones. Front Immunol. 9:3143. Published 2019 Jan 11. doi:10.3389/fimmu.2018.03143 [PubMed: 30687335]

Kfir-Erenfeld S, Yefenof E 2014. Non-genomic events determining the sensitivity of hemopoietic malignancies to glucocorticoid-induced apoptosis. Cancer Immunol Immunother. 63(1):37–43. doi:10.1007/s00262-013-1477-8 [PubMed: 24072402]

Kinoshita Y, Hato F 2001. Cellular and molecular interactions of thymus with endocrine organs and nervous system. Cell Mol Biol (Noisy-le-grand). 47(1):103–117. [PubMed: 11292245]

Kodavanti UP, Ledbetter AD, Thomas RF, Richards JE, Ward WO, Schladweiler MC, et al. 2015. Variability in ozone-induced pulmonary injury and inflammation in healthy and cardiovascular-compromised rat models. Inhal Toxicol. 27 Suppl 1:39–53. doi:10.3109/08958378.2014.954169 [PubMed: 26667330]

Kodavanti UP 2016. Stretching the stress boundary: Linking air pollution health effects to a neurohormonal stress response. Biochim Biophys Acta. 1860(12):2880–2890. doi:10.1016/j.bbagen.2016.05.010 [PubMed: 27166979]

Kodavanti UP 2019. Susceptibility Variations in Air Pollution Health Effects: Incorporating Neuroendocrine Activation. Toxicol Pathol. 47(8):962–975. doi:10.1177/0192623319878402 [PubMed: 31594484]

Koretzky GA 2010. Multiple roles of CD4 and CD8 in T cell activation. J Immunol. 185(5):2643–2644. doi:10.4049/jimmunol.1090076 [PubMed: 20724729]

Krausgruber T, Fortelny N 2020. Fife-Gernedl V, et al. Structural cells are key regulators of organ-specific immune responses. Nature. 583(7815):296–302. doi:10.1038/s41586-020-2424-4 [PubMed: 32612232]

Krüger K, Mooren FC 2014. Exercise-induced leukocyte apoptosis. Exerc Immunol Rev. 20:117–134. [PubMed: 24974724]

Landrigan PJ, Fuller R, Acosta NJR, Adeyi O, Arnold R, Nil Basu N, et al. 2018. The Lancet Commission on pollution and health. Lancet. 391(10119):462–512. [PubMed: 29056410]

Li AF, Richters A 1991. Ambient level ozone effects on subpopulations of thymocytes and spleen T lymphocytes. Arch Environ Health. 46(1):57–63. doi: 10.1080/00039896.1991.9937430. PMID: 1992934. [PubMed: 1992934]

Méndez-Ferrer S, Lucas D, Battista M, Frenette PS 2008. Haematopoietic stem cell release is regulated by circadian oscillations. Nature. 452(7186):442–447. doi:10.1038/nature06685 [PubMed: 18256599]

Miller AH, Spencer RL, hassett J, Kim C, Rhee R, Ciurea D, et al. 1994. Effects of selective type I and II adrenal steroid agonists on immune cell distribution. Endocrinology;135(5):1934–1944. doi:10.1210/endo.135.5.7956914 [PubMed: 7956914]

Miller DB, Karoly ED, Jones JC, Ward WO, Vallanat BD, Andrews DL, et al. 2015. Inhaled ozone (O3)-induces changes in serum metabolomic and liver transcriptomic profiles in rats. Toxicol Appl Pharmacol. 286(2):65–79. doi:10.1016/j.taap.2015.03.025 [PubMed: 25838073]

Miller DB, Ghio AJ, Karoly ED, Bell LN, Snow SJ, Madden MC, et al. 2016a. Ozone Exposure Increases Circulating Stress Hormones and Lipid Metabolites in Humans. Am J Respir Crit Care Med. 193(12):1382–1391. doi:10.1164/rccm.201508-1599OC [PubMed: 26745856]

Miller DB, Snow SJ, Schladweiler MC, Richards JE, Ghio AJ, Ledbetter AD, et al. 2016b. Acute Ozone-Induced Pulmonary and Systemic Metabolic Effects Are Diminished in Adrenalectomized Rats. Toxicol Sci.150(2):312–322. doi:10.1093/toxsci/kfv331 [PubMed: 26732886]

Münzel T, Sørensen M, Gori T, Schmidt FP, Rao X, Brook FR, et al. 2017. Environmental stressors and cardio-metabolic disease: part II-mechanistic insights. Eur Heart J. 38(8):557–564. doi:10.1093/eurheartj/ehw294 [PubMed: 27460891]

Nicholson LB 2016. The immune system. Essays Biochem. 60(3):275–301. doi:10.1042/EBC20160017 [PubMed: 27784777]

Opferman J 2008. Apoptosis in the development of the immune system. Cell Death Differ 15:234–242. 10.1038/sj.cdd.4402182 [PubMed: 17571082]

Padro CJ, Sanders VM 2014. Neuroendocrine regulation of inflammation. Semin Immunol. 26(5):357–368. doi:10.1016/j.smim.2014.01.003 [PubMed: 24486056]

Priftis KN, Chrousos GP 2009. Neuroimmunomodulation in asthma: focus on the hypothalamic-pituitary-adrenal axis. Introduction. Neuroimmunomodulation. 16(5):263–264. doi:10.1159/000216183 [PubMed: 19571586]

Reich C, Dunning WF, 1943. Studies on the morphology of peripheral blood in rats. I. Normal rats. Cancer Res. 3 : 248–257.

Ritchie AI, Singanayagam A, Wiater E, Edwards MR, Montminy M, Johnston SL 2018. β_2-Agonists Enhance Asthma-Relevant Inflammatory Mediators in Human Airway Epithelial Cells. Am J Respir Cell Mol Biol. 58(1):128–132. doi:10.1165/rcmb.2017-0315LE [PubMed: 29286858]

Ritchie H, Roser M 2020 - "Outdoor Air Pollution". Published online at OurWorldInData.org. Retrieved May 1, 2020 from: https://ourworldindata.org/outdoor-air-pollution' [Online Resource]

Sanders VM. Kasprowicz DJ Kohm AP Swanson MA 2001. Neurotransmitter receptors on lymphocytes and other lymphoid cells. In: Ader R; Felten D; Cohen, editors. Psychoneuroimmunology. 3rd. San Diego,CA: Academic Press. p. 161–196.

Savino W, Mendes-da-Cruz DA, Lepletier A, Dardenne M 2016. Hormonal control of T-cell development in health and disease. Nat Rev Endocrinol. 12(2):77–89. doi:10.1038/nrendo.2015.168 [PubMed: 26437623]

Scapellato ML, Lotti M 2007. Short-term effects of particulate matter: an inflammatory mechanism?. Crit Rev Toxicol. 37(6):461–487. doi:10.1080/10408440701385622 [PubMed: 17661213]

Shannahan JH, Schladweiler MC, Richards JH, Ledbetter AD, Ghio AJ, Kodavanti UP 2010. Pulmonary oxidative stress, inflammation, and dysregulated iron homeostasis in rat models of cardiovascular disease. J Toxicol Environ Health A. 73(10):641–656. doi:10.1080/15287390903578208. [PubMed: 20391109]

Snow SJ, Henriquez AR, Costa DL, Kodavanti UP 2018. Neuroendocrine Regulation of Air Pollution Health Effects: Emerging Insights. Toxicol Sci.164(1):9–20. doi:10.1093/toxsci/kfy129 [PubMed: 29846720]

Steenhof M, Janssen NA, Strak M, Hoek G, Gosens I, Mudway IS, et al. 2014. Air pollution exposure affects circulating white blood cell counts in healthy subjects: the role of particle composition, oxidative potential and gaseous pollutants - the RAPTES project. Inhal Toxicol. 26(3):141–165. doi:10.3109/08958378.2013.861884 [PubMed: 24517839]

Steer JH, Kroeger KM, Abraham LJ, Joyce DA 2000. Glucocorticoids suppress tumor necrosis factor-alpha expression by human monocytic THP-1 cells by suppressing transactivation through adjacent NF-kappa B and c-Jun-activating transcription factor-2 binding sites in the promoter. J Biol Chem. 275(24):18432–18440. doi:10.1074/jbc.M906304199 [PubMed: 10748079]

U.S. EPA. 2020. Integrated Science Assessment (ISA) for Ozone and Related Photochemical Oxidants (Final Report). U.S. Environmental Protection Agency, Washington, DC, EPA/600/R-20/012, 2020.

van Eeden SF, Yeung A, Quinlam K, Hogg JC 2005. Systemic response to ambient particulate matter: relevance to chronic obstructive pulmonary disease. Proc Am Thorac Soc. 2(1):61–67. doi:10.1513/pats.200406-035MS [PubMed: 16113470]

Wiechmann T, Röh S, Sauer S, Czamara D, Arloth J, Ködel M, et al. 2019. Identification of dynamic glucocorticoid-induced methylation changes at the FKBP5 locus. Clin Epigenetics. 11(1):83. Published 2019 May 23. doi:10.1186/s13148-019-0682-5. [PubMed: 31122292]

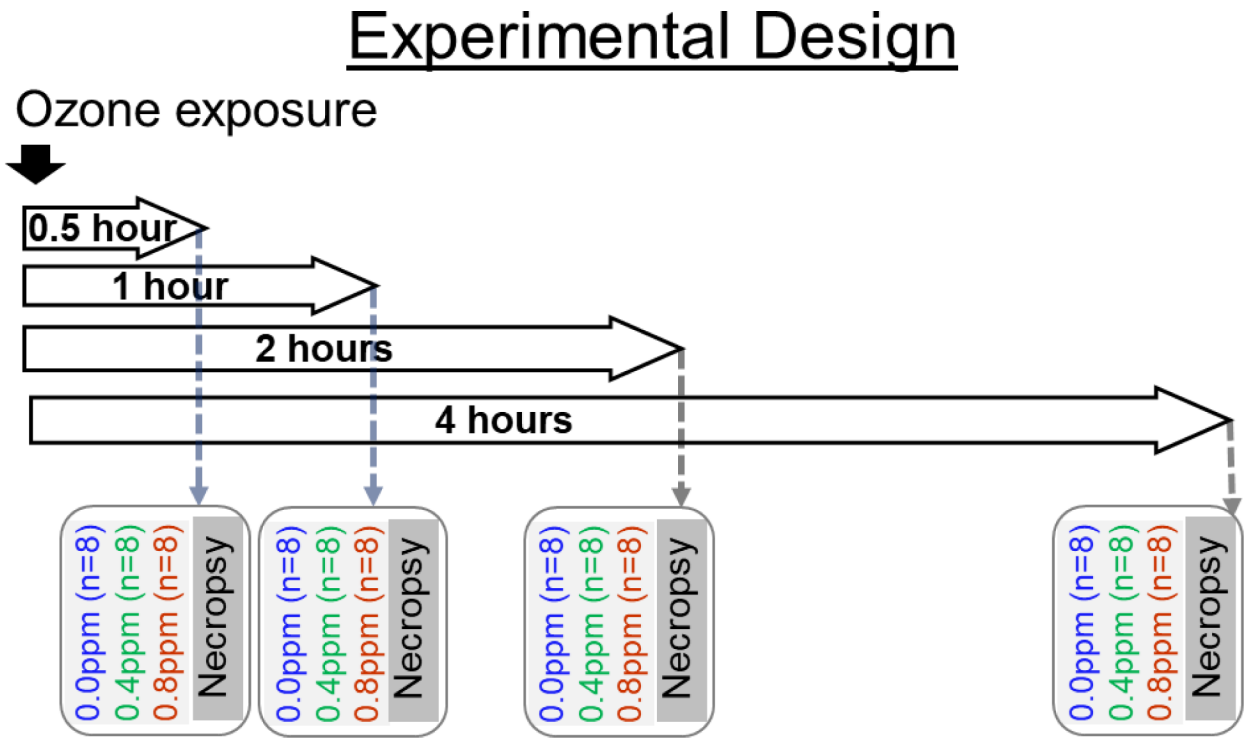

Figure 1.

Schema of the experimental design. The times of air or ozone exposures (horizontal), and necropsies (vertical) are indicated by arrows. Different sets of animals for each time point of 0.5, 1, 2 or 4 hours were exposed to air (0.0 ppm ozone), or 0.4 or 0.8 ppm ozone. Eight animals per group (for each exposure/time) were analyzed totaling 24 rats per timepoint. Tissue collection was performed within 20 min once exposure was terminated.

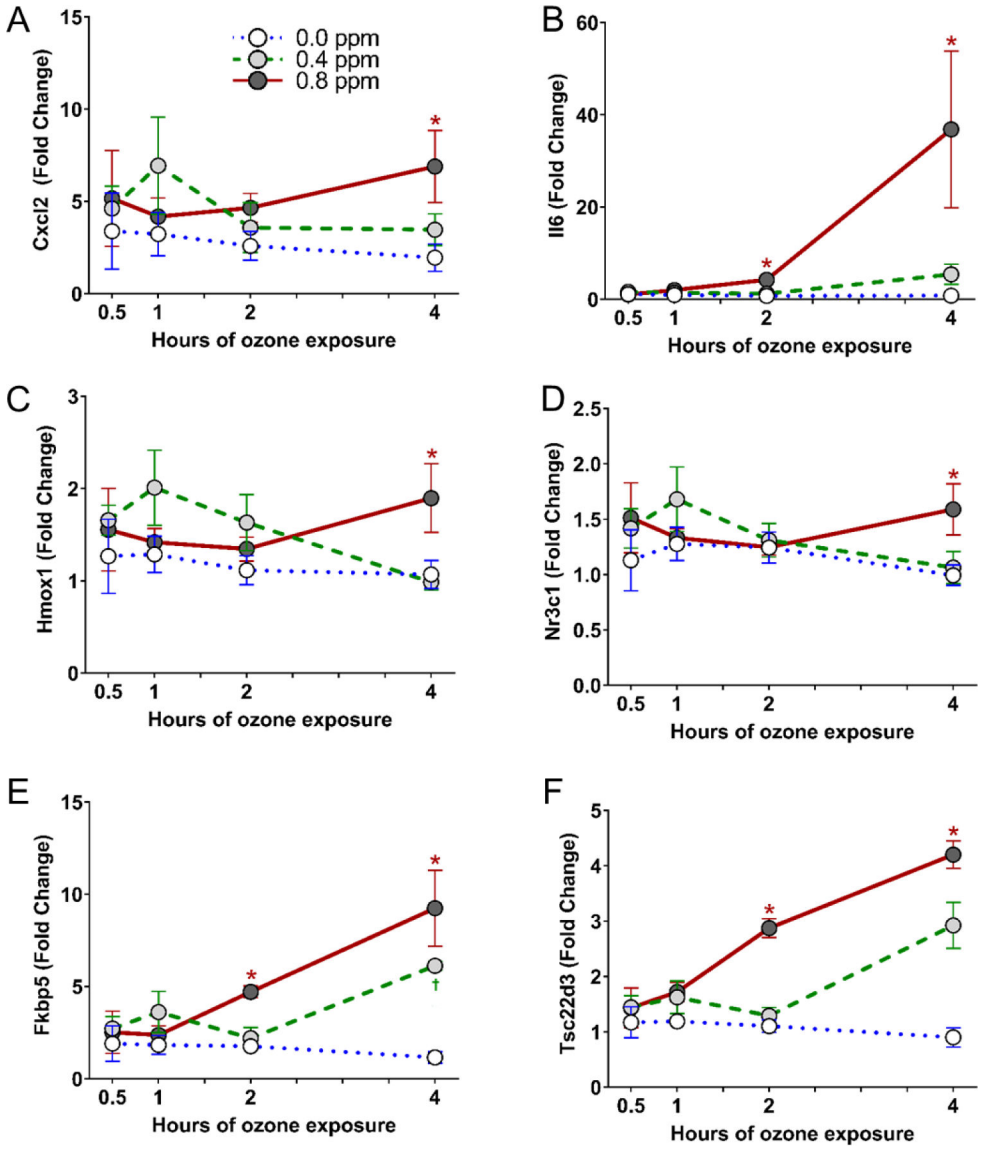

Figure 2.

The time course of inflammatory and glucocorticoid responsive gene expression in the lung at various times over 4-hr ozone exposure. The data show mean ± SE of n=6–8 rats/group. *Significant ozone effect ($P \leq 0.05$) at 0.8 ppm relative to time-matched air group; †significant ozone effect at 0.4 ppm relative to time-matched air group. Cxcl2, Chemokine (C-X-C motif) ligand 2 (A); Il6, interleukin 6 (B); Hmox1, heme oxygenase 1 (C); Nr3c1, Nuclear receptor subfamily 3 group c member 1, glucocorticoid receptor (D); Fkbp5, FK506 binding protein 5, a co-chaperone of the glucocorticoid receptor (E); Tsc22d3, TSC22 domain family protein 3, glucocorticoid-induced gene (F).

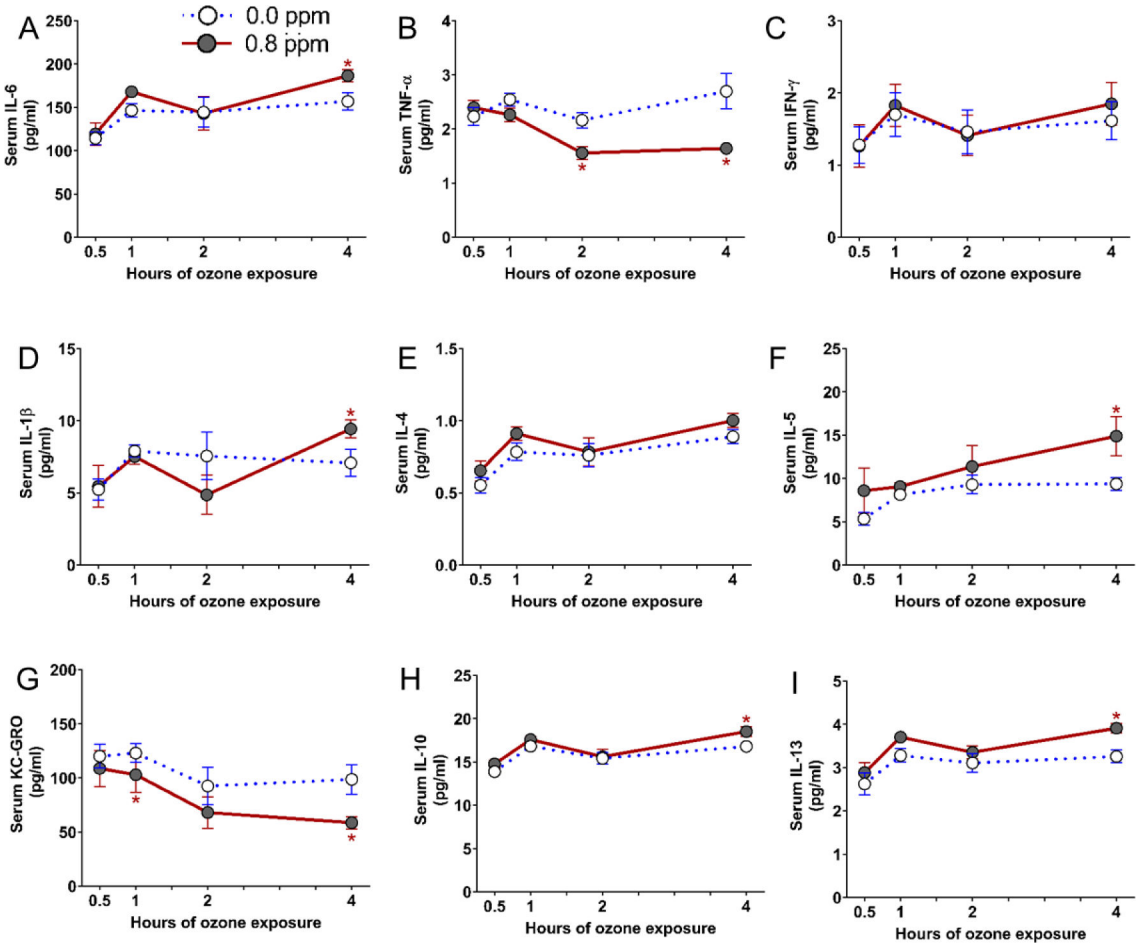

Figure 3.

Changes in circulating cytokines over the course of 4 hours 0.8 ppm ozone exposure in rats. The data show mean ± SE of n=6–8 rats/group. *Significant ozone effect ($P \leq 0.05$) at 0.8 ppm relative to time-matched air group. (A) IL-6, interleukin-6; (B) TNF-α, tumor necrosis factor α; (C) IFN-γ, interferon-γ; (D) IL-1β, interleukin-1β; (E) IL-4, interleukin-4; (F) IL-5, interleukin-5; (G) KC-GRO, keratinocyte chemoattractant/human growth-regulated oncogene; (H) IL-10, interleukin-10; (I) IL-13, interleukin-13.

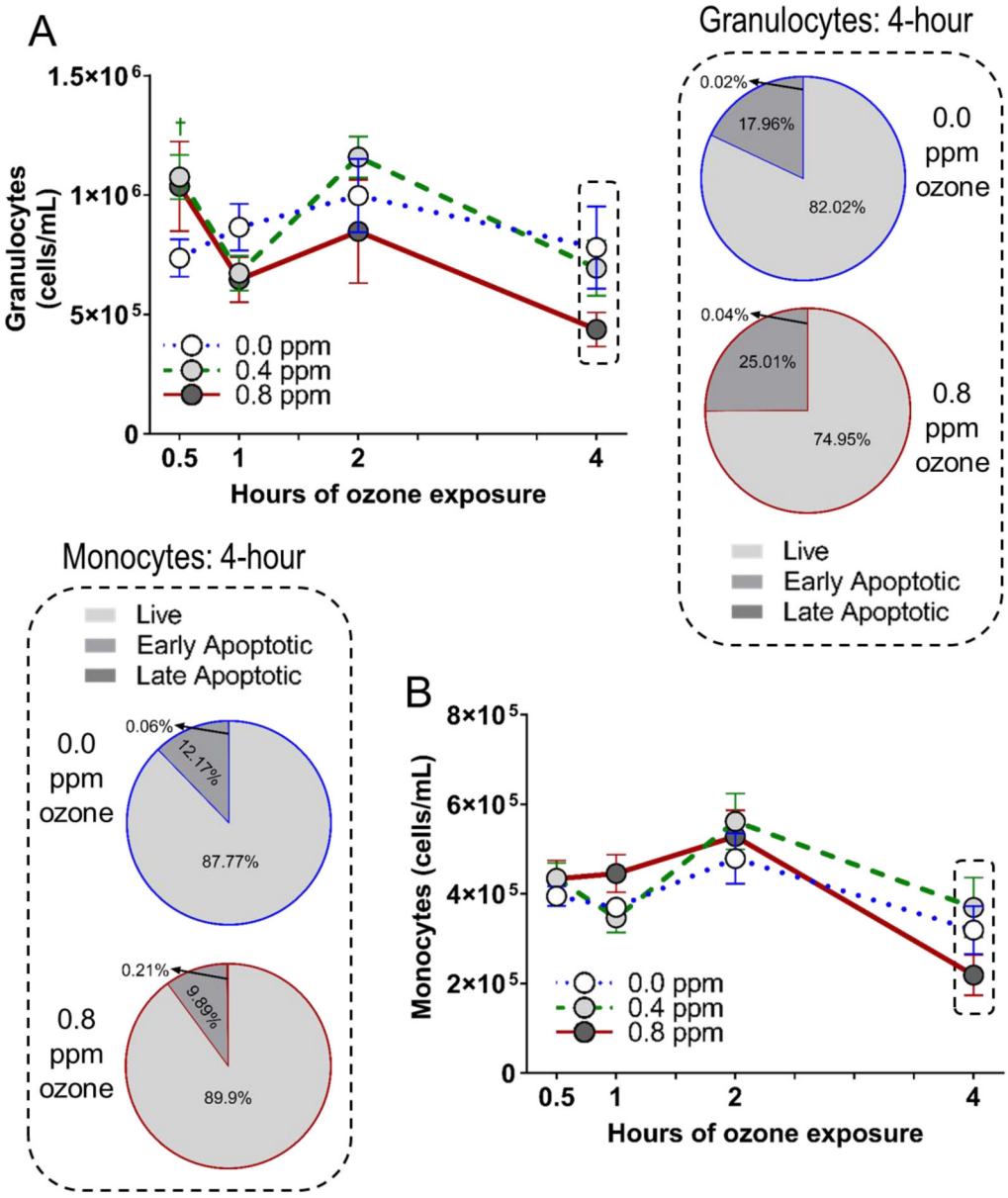

Figure 4.

The time-course of ozone-induced changes in total circulating granulocytes (A) and monocytes (B) over a 4 hour exposure period and their viability at 4-hour time point. The pie charts show % of live cells versus early apoptotic and late apoptotic cells at 4-hour time point for air and 0.8 ppm ozone groups. Note that in some cases no cells were detected undergoing apoptosis or necrosis for which zero values were assigned. The data show mean ± SE of n=6–8 rats/group. †Significant ozone effect at 0.4 ppm relative to time-matched air group ($P \leq 0.05$).

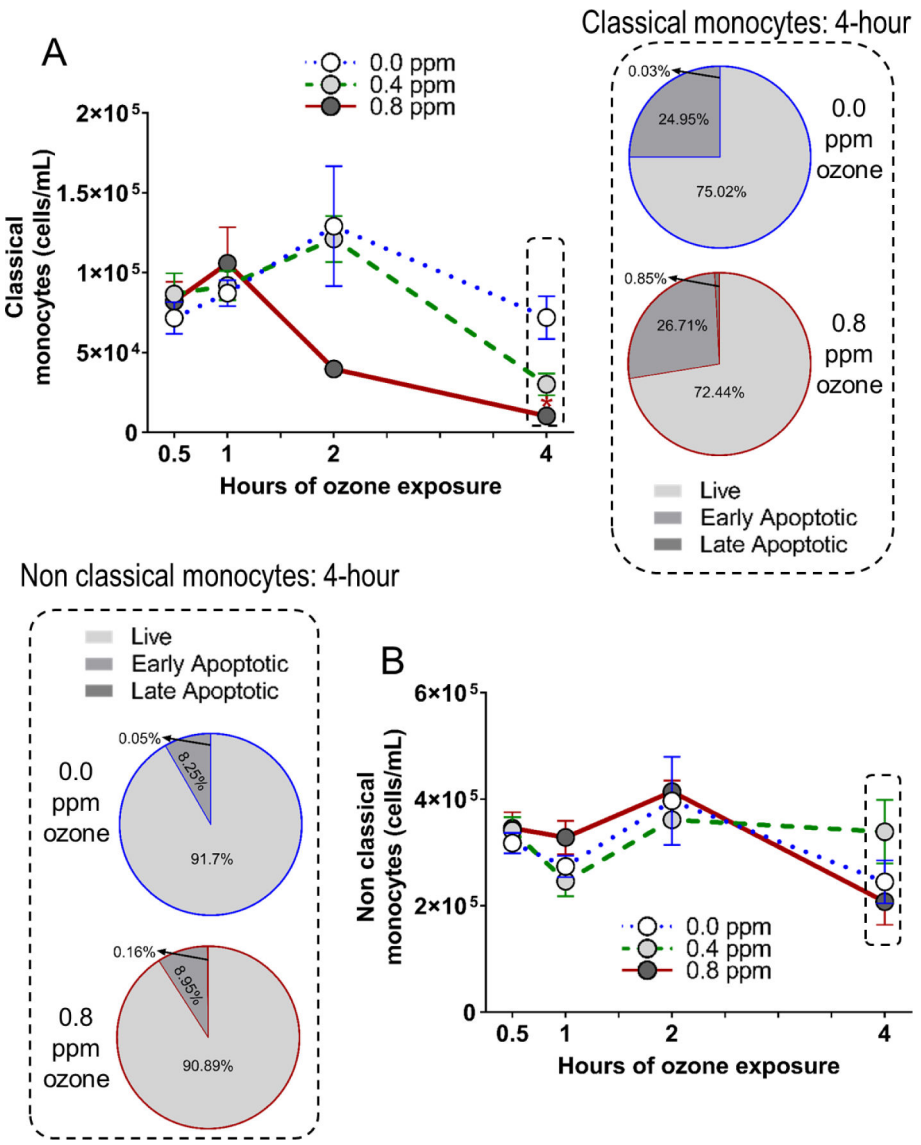

Figure 5.

The time-course of ozone-induced changes in circulating classical (A) and non-classical (B) monocytes over a 4-hour exposure period and their viability at 4-hour time point. The pie charts show % of live cells versus early apoptotic and late apoptotic cells at 4-hour time point for air and 0.8 ppm ozone groups. The data show mean ± SE of n=6–8 rats/group for 30 min, 1-hour and 4-hour time points. At 2-hour time point, the data for only 2 animals were considered due to an experimental issue in analyzing other samples for monocytes. The 2 -hour time point, therefore, was not considered for statistical analysis of classical and non-classical monocytes. *Significant ozone effect at 0.8 ppm relative to time-matched air group ($P \leq 0.05$).

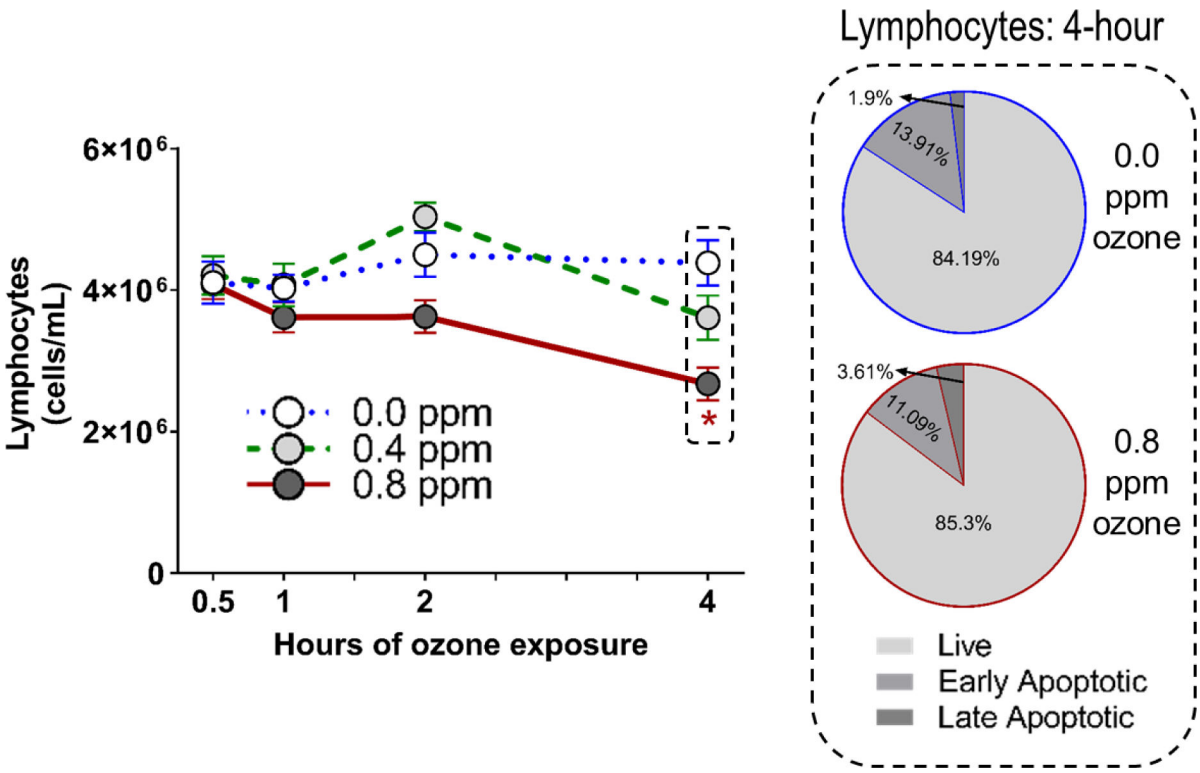

Figure 6.

The time-course of ozone-induced changes in total circulating lymphocytes over a 4-hour exposure period and their viability at 4-hour time point. The pie charts show % of live cells versus early apoptotic and late apoptotic cells at 4-hour time point for air and 0.8 ppm ozone groups. The data show mean ± SE of n=6–8 rats/group. *Significant ozone effect at 0.8 ppm relative to time-matched air group ($P \leq 0.05$).

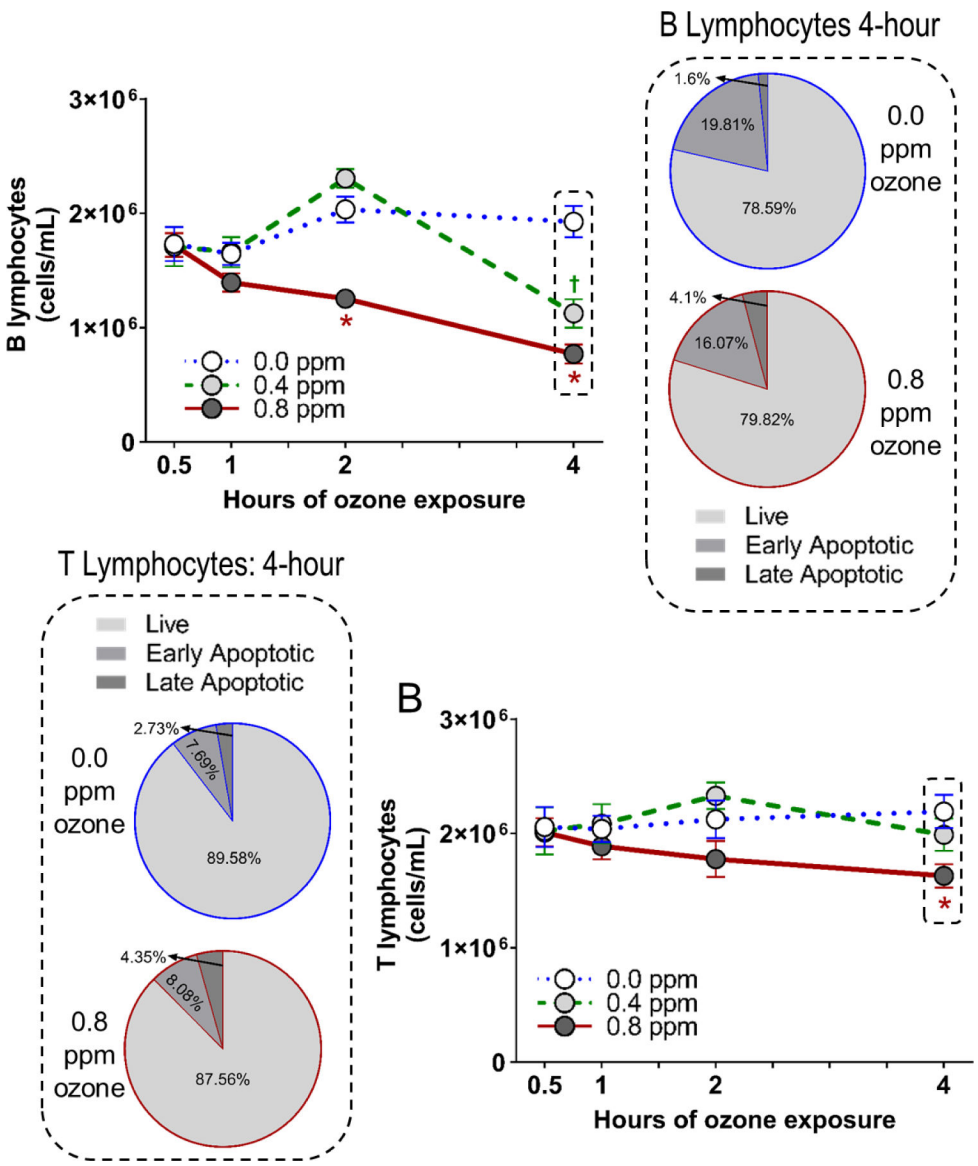

Figure 7.

The time-course of ozone-induced changes in circulating B-lymphocytes (A) and T-lymphocytes (B) over a 4-hour exposure period and their viability at 4-hour time point. The pie charts show % of live cells versus, early apoptotic and late apoptotic cells at 4-hour time point for air and 0.8 ppm ozone groups. The data show mean ± SE of n=6–8 rats/group. *Significant ozone effect ($P \leq 0.05$) at 0.8 ppm relative to time-matched air group; †significant ozone effect at 0.4 ppm relative to time-matched air group.

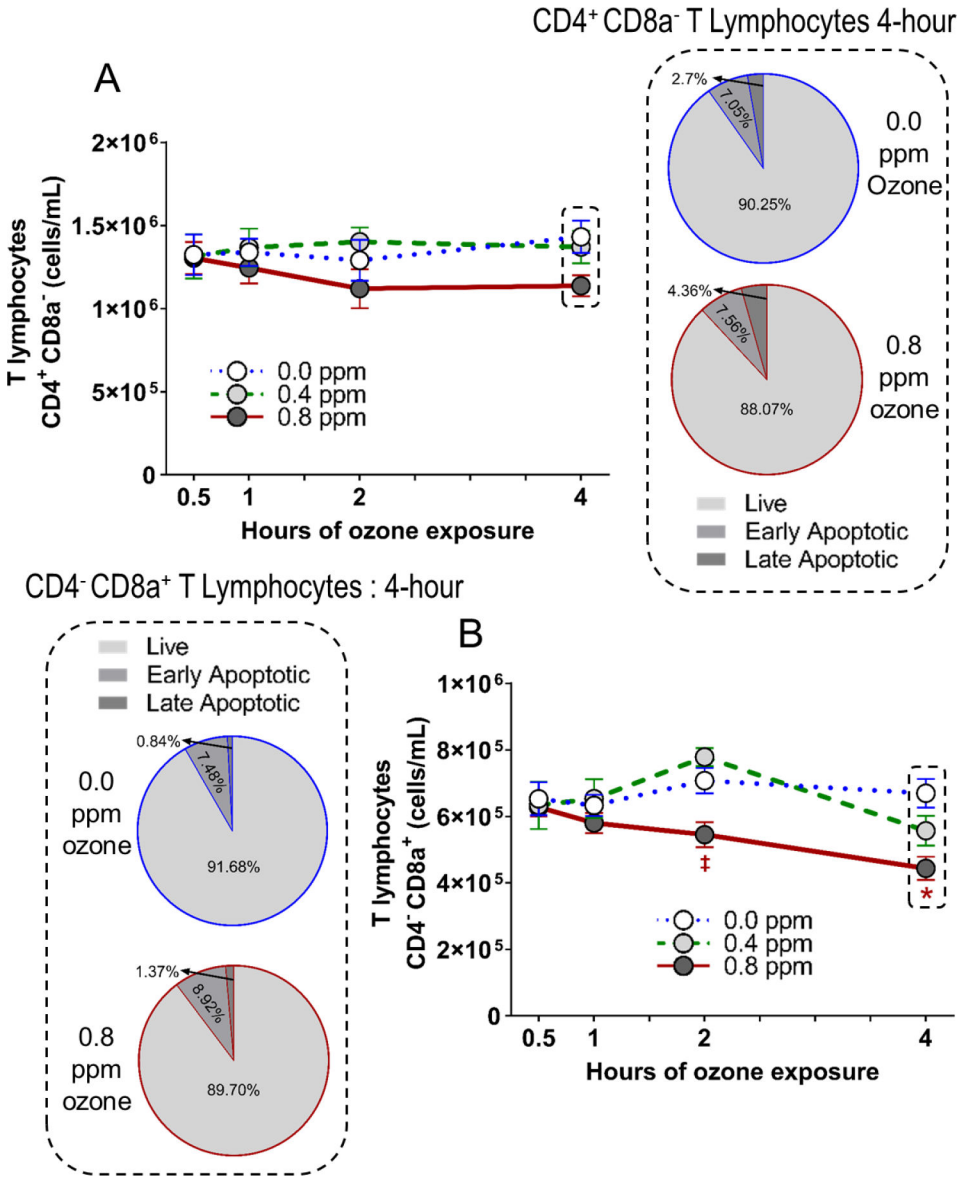

Figure 8.

The time-course of ozone-induced changes in circulating T helper (CD4+ CD8a−; A) and T cytotoxic lymphocytes (CD4+ CD8a−; B) over a 4-hr exposure period and their viability at 4-hour time point. The pie charts show % of live cells, early apoptotic and late apoptotic cells at 4-hour time point for air and 0.8 ppm ozone groups. The data show mean ± SE of n=6–8 rats/group. *Significant ozone effect at 0.8 ppm relative to time-matched air group ($P \leq 0.05$).

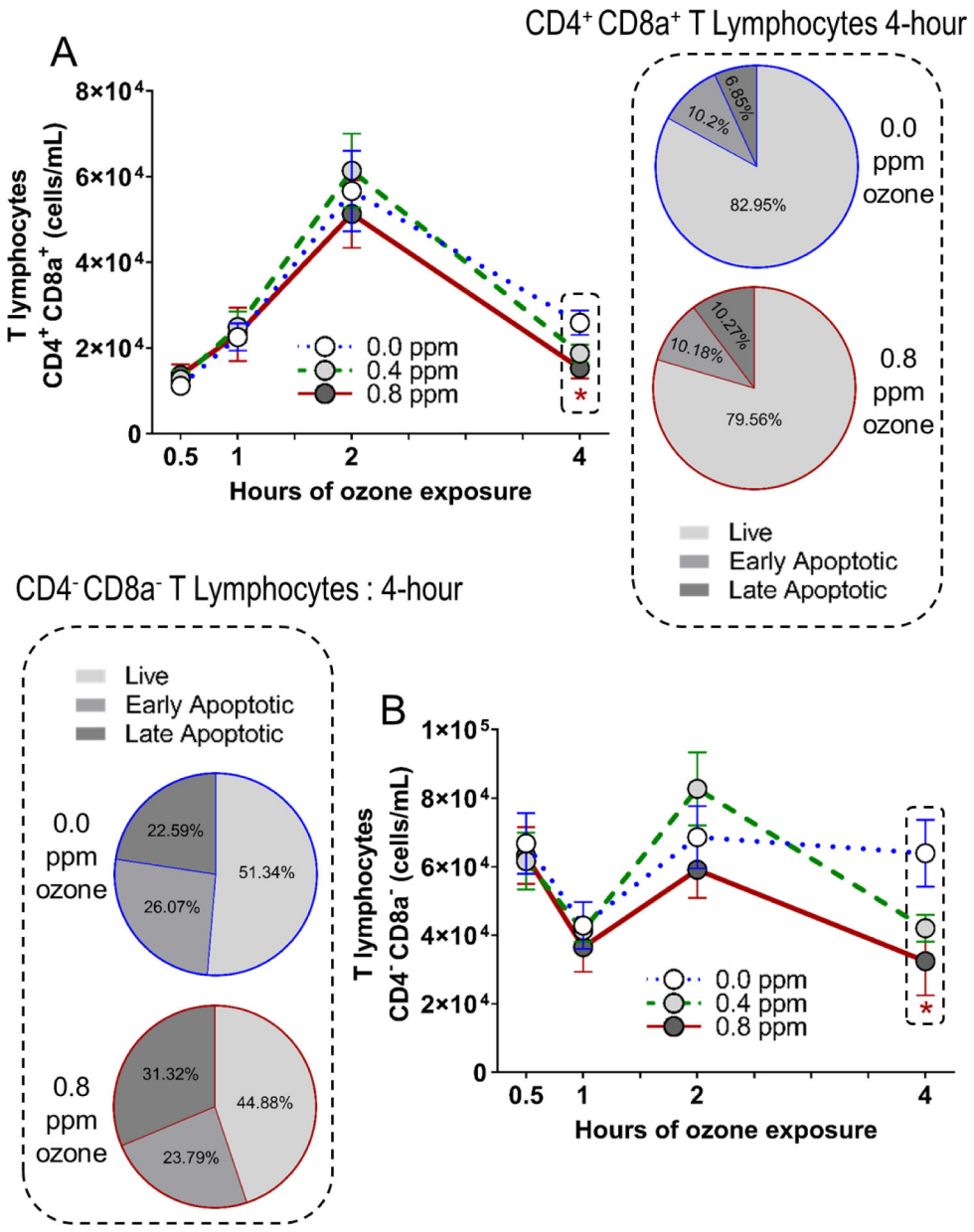

Figure 9.

The time-course of ozone-induced changes in circulating CD4+ CD8a+ and CD4− CD8a− lymphocytes over a 4-hour exposure period and their viability at 4-hour time point. The pie charts show % of live cells versus, early apoptotic and late apoptotic cells at 4-hour time point for air and 0.8 ppm ozone groups. The data show mean ± SE of n=6–8 rats/group. *Significant ozone effect at 0.8 ppm relative to time-matched air group ($P \leq 0.05$).

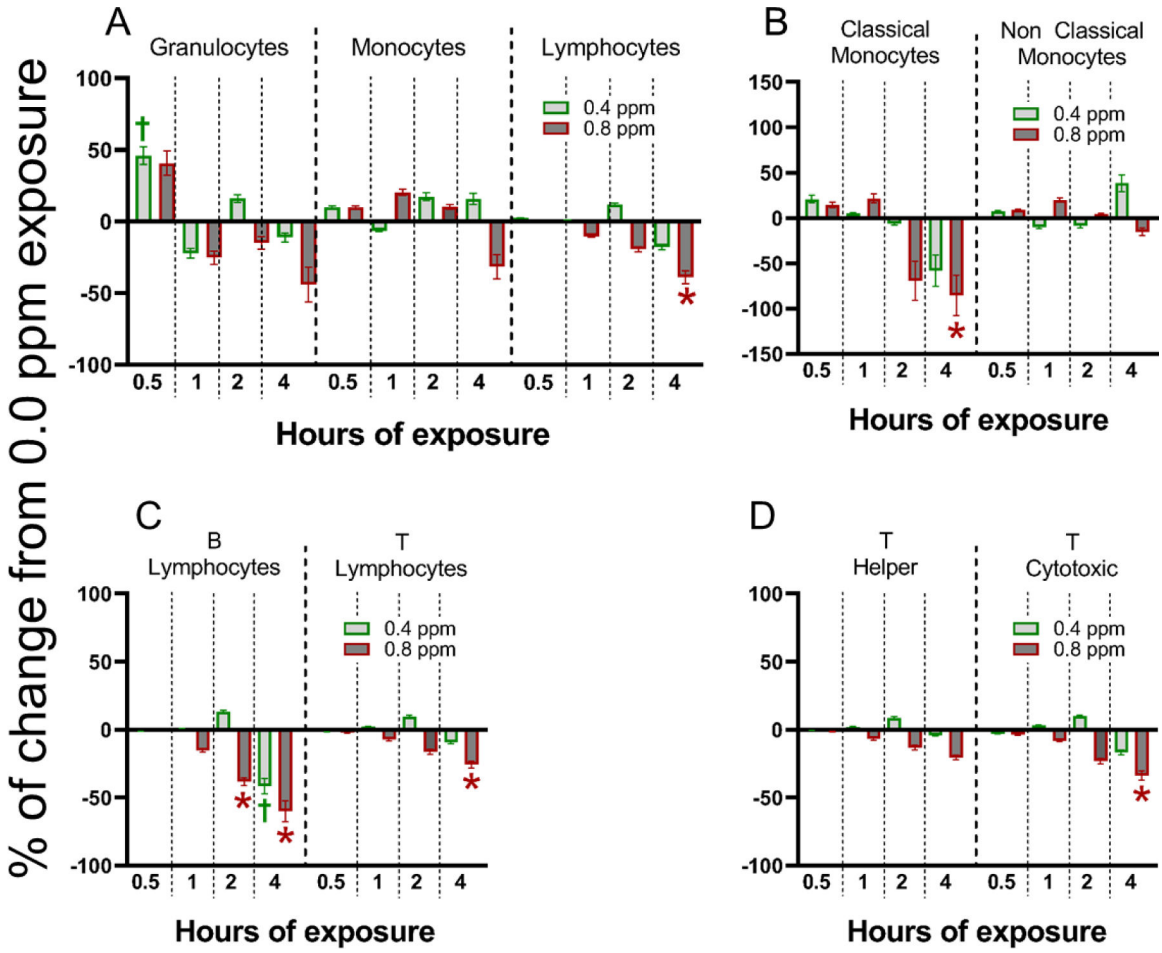

Figure 10.

Summary bar graphs showing time-related changes (%) in circulating granulocyte subpopulations after exposure to 0.4 or 0.8 ppm ozone. Bar graphs show % change from air group for different cell populations. The data show mean ± SE of n=6–8 rats/group. *Significant ozone effect ($P \leq 0.05$) at 0.8 ppm relative to time-matched air group; †significant ozone effect at 0.4 ppm relative to time-matched air group.

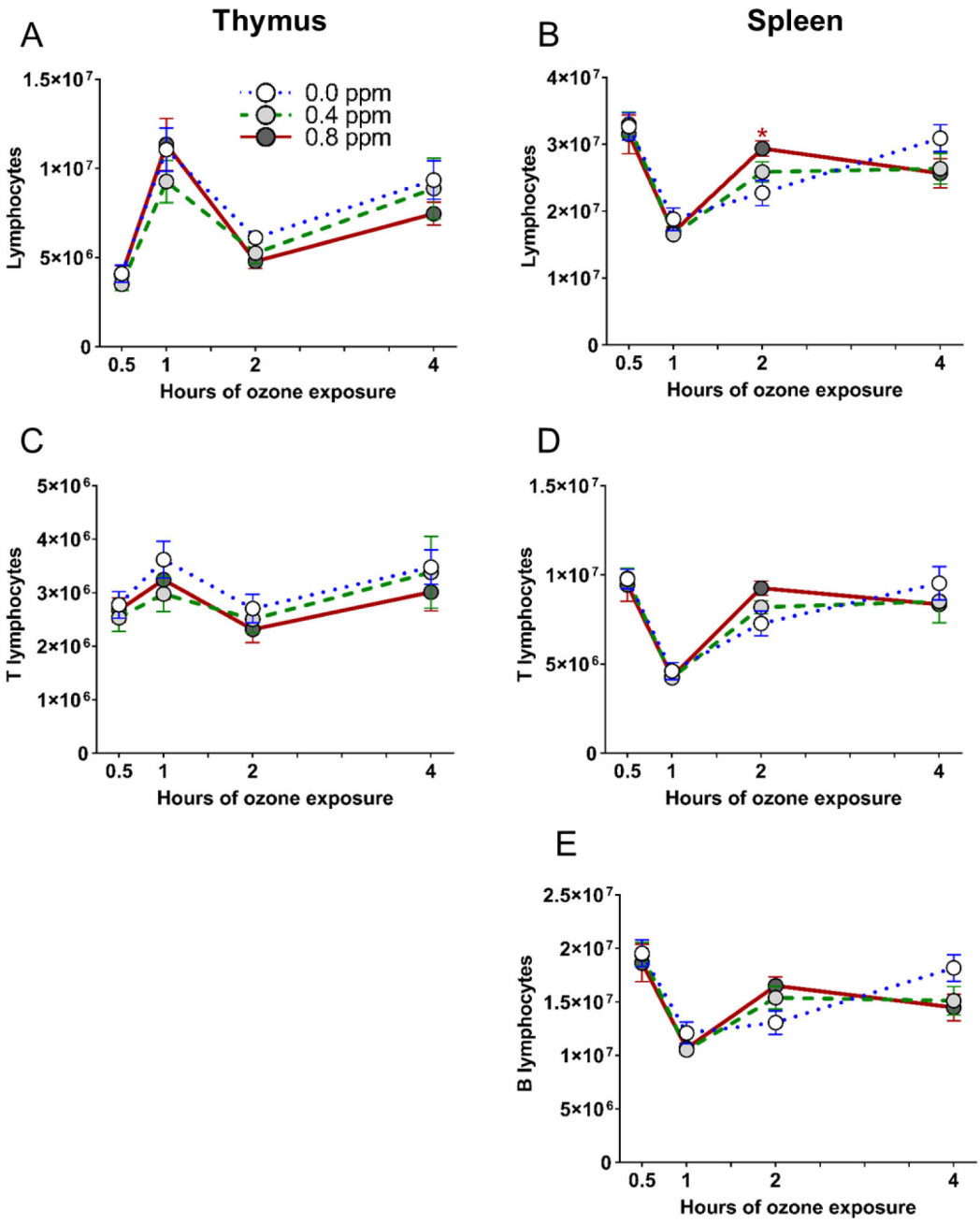

Figure 11.

The time-course of ozone-induced changes in thymus lymphocytes (A) and T lymphocytes (B); and spleen lymphocytes (C), T lymphocytes (D) and B lymphocytes (E) over a 4-hour exposure period. The data show mean ± SE of n=6–8 rats/group. *Significant ozone effect ($P \leq 0.05$) at 0.8 ppm relative to time-matched air group.

Table 1.

The list of labelled antibodies, their source and dilutions used for identification of cells with different surface markers in blood, thymus and spleen.

	Antibody or dye and fluorochrome	Clone	Lot #	Isotype Control	Lot #	Dilution
Blood (1st aliquot)	CD45-Vioblue	REA504	5170929136	REA Control-VioBlue	5170929097	0.15 μg / 10^6 cells
	CD11b/c-PE-Vio770	REA325	5170315710	REA Control-PE-Vio770	5170929099	0.15 μg / 10^6 cells
	CD172a-PE	REA490	5170929108	REA Control-PE	5170814844	0.15 μg / 10^6 cells
	CD43-APC	REA503	5170929109	REA Control-APC	5170922339	0.15 μg / 10^6 cells
Blood (2nd aliquot)	CD45-Vioblue	REA504	5170929136	REA Control-VioBlue	5170929098	0.15 μg / 10^6 cells
	CD3-PE	REA223	5170929093	REA Control-PE	5170814844	0.15 μg / 10^6 cells
	CD4-PerCP-Vio700	REA482	5170929107/ 5170530082	REA Control-PerCP-Vio700	5170929100	0.15 μg / 10^6 cells
	CD8a-VioGreen	REA437	5170929112	REA Control-VioGreen	5170929097	0.15 μg / 10^6 cells
	CD45R-APC	REA450	5170929103	REA Control-APC	5170922339	0.15 μg / 10^6 cells
Thymus	CD45-Vioblue	REA504	5170929136	REA Control-VioBlue	5170929098	0.15 μg / 10^6 cells
	CD3-PE	REA223	5170929093	REA Control-PE	5170814844	0.15 μg / 10^6 cells
	CD4-PerCP-Vio700	REA482	5170929107/ 5170530082	REA Control-PerCP-Vio700	5170929100	0.15 μg / 10^6 cells
	CD8a-VioGreen	REA437	5170929112	REA Control-VioGreen	5170929097	0.15 μg / 10^6 cells
Spleen	CD45-Vioblue	REA504	5170929136	REA Control-VioBlue	5170929098	0.15 μg / 10^6 cells
	CD3-PE	REA223	5170929093	REA Control-PE	5170814844	0.15 μg / 10^6 cells
	CD4-PerCP-Vio700	REA482	5170929107 / 5170530082	REA Control-PerCP-Vio700	5170929100	0.15 μg / 10^6 cells
	CD8a-VioGreen	REA437	5170929112	REA Control-VioGreen	5170929097	0.15 μg / 10^6 cells
	CD45R-APC	REA450	5170929103	REA Control-APC	5170922339	0.15 μg / 10^6 cells
For all tissues	Fixable Viability Dye eFluor™ 780	-	-	-	-	1 uL / 10^6 cells
	Annexin V - FITC Apoptosis Detection Kit	-	-	-	-	5 uL / 10^6 cells

All materials were obtained from Miltenyi Biotec Inc (Somerville, MA, USA) except for Dye eFluor™ 780 and Apoptosis Detection Kit, which were obtained from Thermo Fisher Scientific (Waltham, MA).

Table 2.

Cell surface markers used to identify blood, thymus and spleen leukocytes.

Blood Panel							
First aliquot							
CD45+	Leukocytes	Hi SSC-A	Granulocytes				
		CD172+ CD11b/c+	Monocytes	CD43 Low	Classical		
				CD43 High	Non Classical		
Second aliquot							
CD45+	Leukocytes	Low SSC-A	Lymphocytes	CD45R+	B lymphocytes		
				CD3+	T lymphocytes	CD4+ CD8a+	
						CD4+ CD8a−	T helper
						CD4− CD8a+	T cytotoxic
						CD4− CD8a−	
Thymus Panel							
CD45+	Leukocytes	Low SSC-A	Lymphocytes	CD3+	T lymphocytes	CD4+ CD8a+	
						CD4+ CD8a−	T helper
						CD4− CD8a+	T cytotoxic
						CD4− CD8a−	
Spleen Panel							
CD45+	Leukocytes	Low SSC-A	Lymphocytes	CD45R+	B lymphocytes		
				CD3+	T lymphocytes	CD4+ CD8a+	
						CD4+ CD8a−	T helper
						CD4− CD8a+	T cytotoxic
						CD4− CD8a−	

Marker antibodies used in flow cytometry for the isolation and separation of different cell populations from blood, thymus and spleen. A separate aliquot of blood cells was used for isolating granulocytes/monocytes and lymphocytes. Whole thymus and spleen tissues were digested to isolate cells. All cells were assessed for viability and apoptosis status.

Table 3.

The changes in plasma epinephrine and corticosterone levels over time in rats exposed to ozone.

	Plasma Epinephrine (pg/mL)			Plasma Corticosterone (ng/mL)		
Ozone→	**0.0 ppm**	**0.4 ppm**	**0.8 ppm**	**0.0 ppm**	**0.4 ppm**	**0.8 ppm**
0.5hr	57.4 ± 7.0	50.0 ± 7.1	69.3 ± 13.4	319.0 ± 62.5	243.8 ± 28.2	521.7 ± 129.5
1hr	54.1 ± 4.9	63.9 ± 9.1	100.2 ± 15.8*	443.3 ± 85.5	459.3 ± 86.5	1182.0 ± 147.1*
2hr	50.9 ± 9.1	81.5 ± 15.1	113.6 ± 18.7*	310.8 ± 53.0	273.8 ± 27.4	932.8 ± 125.4*
4hr	44.2 ± 8.4	112.7 ± 45.0†	123.4 ± 36.9*	320.5 ± 64.1	1386.6 ± 214.4†	876.8 ± 161.6*

Rats were exposed to ozone for 30 minutes, 1 hour, 2 hour or 4 hour and immediately following exposure blood and tissue samples were collected. Data show mean ± Standard error (n=5–6/group).

*Significant ozone effect ($P \leq 0.05$) at 0.8 ppm relative to time-matched air group

†significant ozone effect at 0.4 ppm relative to time-matched air group.